Summer 8-12-2016

A Comparative Analysis of Nicotinic Acetylcholine Receptor Subunits and Cholinergic Neurons in Nudipleura Molluscs

Seydanur Tikir

Summer 8-12-2016

A COMPARATIVE ANALYSIS OF NICOTINIC ACETYLCHOLINE RECEPTOR SUBUNITS AND CHOLINERGIC NEURONS IN NUDIPLEURA MOLLUSCS

Seydanur Tikir

A COMPARATIVE ANALYSIS OF NICOTINIC ACETYLCHOLINE RECEPTOR SUBUNITS AND CHOLINERGIC NEURONS IN NUDIPLEURA MOLLUSCS

by

SEYDANUR TIKIR

Under the Direction of Paul S. Katz

ABSTRACT

Acetylcholine (ACh) and nicotinic acetylcholine receptors (nAChR) play important roles in the transmission of electrical signals in the brain. The diversity of nAChR subunits contributes to differential regulation of signal transmission at synapses. Twenty types of nAChR subunits were previously identified in two gastropod molluscs, *Aplysia californica* and *Lymnaea stagnalis* (van Nierop et al., 2006; White et al., 2014). Here, they were identified in six nudipleura molluscs: *Flabellina iodinea, Hermissenda crassicornis, Tritonia diomedea, Pleurobranchaea californica, Melibe leonina* and *Dendronotus iris*. In addition, four novel nAChR subunits were predicted with an ortholog-based approach. Bioinformatically determined gene expression levels showed species differences. Whole-mount *in situ* hybridization using choline acetyltransferase gene probes localized cholinergic neurons in the brains of *Dendronotus* and *Melibe*. Investigation and comparison of nAChRs and cholinergic neurons in the brains of these animals will help to understand how neurochemistry relates to the organization and evolution of neural circuitry.

INDEX WORDS: Receptor subunit composition, Transcriptomics, BLAST, Evolution, Choline acetyltransferase, Nudibranch

A COMPARATIVE ANALYSIS OF NICOTINIC ACETYLCHOLINE RECEPTOR SUBUNITS AND CHOLINERGIC NEURONS IN NUDIPLEURA MOLLUSCS

by

SEYDANUR TIKIR

A Thesis Submitted in Partial Fulfillment of the Requirements for the Degree of

Master of Science

in the College of Arts and Sciences

Georgia State University

2016

A COMPARATIVE ANALYSIS OF NICOTINIC ACETYLCHOLINE RECEPTOR SUBUNITS AND CHOLINERGIC NEURONS IN NUDIPLEURA MOLLUSCS

by

SEYDANUR TIKIR

Committee Chair: Paul S. Katz

Committee: Charles D. Derby

Walter Wilczynski

Electronic Version Approved:

Office of Graduate Studies

College of Arts and Sciences

Georgia State University

August 2016

ACKNOWLEDGEMENTS

Even with the utmost hard work this research would not have been possible without the support of precious individuals. Above all, I would like to acknowledge my advisor, Paul Katz, for the priceless guidance, motivation and support that he provided me. Throughout my degree education, I asked numerous questions to Paul and always enjoyed discussing scientific concepts with him. Paul has always been open to my ideas, even to the craziest ones. He has the habit of guiding me in just the correct way. If I was given with the opportunity to address the crowd in Academy Awards, I would definitely honor Paul with the best PI of the year award. Dear Paul, thank you for believing in me, besides everything else you did.

Thanks to the members of my thesis committee, Charles Derby and Walter Wilczynski, for their great advices, suggestions and support. Thank you to my master's program coordinator Bill Walthall. You've always been so helpful and nice.

Many thanks goes to Akira Sakurai, the electro physiology maestro of our lab, for helping me in my double labeling in situ hybridization experiments with filling cells.

I would like to acknowledge Rachael Beaumont for starting the studies of nicotnic acetylcholine receptors in our lab. She started working in our lab as a high school ION student, and I mentored her to identify twelve acetylcholine receptors with BLAST searches. Her findings has verified a part of my results.

Special thanks to my friend Dilara for supporting me whenever I need. I very most enjoyed brainstorming with her. We teamed up with our the power of molecular biology and computer science.

Many thanks to my friend Ulkuhan, who was my cheerful companion during my overnight studying sessions.

My special thanks are to my dearest friends Busra, Nursen, Elif, Banu, Cemile, and Thaksila for giving me their supports.

I cannot forget the contributions of Dr. Thomas Girke to my education in Bioinformatics, who provided me with the opportunity of interning in his lab in the summer of 2012. Learning how to do next-generation data analysis in his lab significantly helped me on my thesis research.

When I think of a “mentor”, Ahmet Rasit Ozturk comes to my mind. I started my journey in Bioinformatics while interning at his company at Bilkent University Cyberpark. He has been a role model to me with his great energy, originality and vision. I always remember him and his wife Melike as sincere friends, as well as a big sister and big brother who guided me. They continuously motivated me to follow my dreams.

I would also want to thank you, a number of past and current members of the Katz Lab: Aastha, Akira, Amirah, Arianna, Charuni, Elif, Jonathan, Megan, Preetham, Saba, Rachael, and Ryan. You have been good friends and colleagues to me. I always enjoyed having conversations with you in the lab or during our lab meetings.

Many thanks to Adriano Senatore for showing me the art of making experiments, and sharing his valuable experiences in academia with me. Adriano is the one who encouraged me for going after my creativity. I owe my intuition towards creating better and new protocols to him.

I would like to send my special thanks to the fantastic employees in the department of Biology and Neuroscience: Claudia, Latesha and Tracy. They have been extremely helpful in anything that I asked from them.

Thanks to Stephanie Gutzler for providing me with a teaching assistantship opportunity.

Over the two years of my master's study, I had the opportunity to attend the lectures of amazing scientists. Many thanks to Gennady Cymbalyuk, Anne Murphy, Dan Cox, Sunayana Banerjee, Matthew Grober and Aaron Gregory Roseberry.

I would like to acknowledge beautiful sea slugs for swimming so beautifully and uniquely, for possessing giant neurons to work on, and for having simple neural circuits to work with. No other organism could have provide such a great platform for answering the great scientific questions of the Katz lab.

Lastly but most importantly, thank you, my family, for always supporting me. I always appreciated your support for me. I would like to thank my lovely nieces and nephews, Sena, Esma Zulal, Ahmet Eymen, and Betul, for always bringing a smile to my face.

TABLE OF CONTENTS

LIST OF TABLES

LIST OF FIGURES

1 CHAPTER 1: NICOTINIC ACETYLCHOLINE RECEPTORS

1.1 INTRODUCTION

1.1.1 The goal of this chapter

In this chapter, nicotinic acetylcholine receptor (nAChR) subunit sequences are analyzed in six nudipleurans: *Flabellina, Hermissenda, Tritonia, Pleurobranchaea, Melibe* and *Dendronotus*. The sequences of the subunits, their similarity, and expression levels are highlighted. The main phylogenetic relations between nAChR subunits are resolved.

1.1.2 Introduction to nAChRs and their structure

Ion channels and receptors are key to synaptic transmission in all animals with nervous systems. The receptors that are gated with acetylcholine (ACh) consist of two main classes: nicotinic and muscarinic ACh receptors (AChRs). Muscarinic ACh receptors (mAChR) are G-protein-coupled-receptors (GPCRs) that are gated muscarine and ACh, whereas the nAChRs are ligand gated ion channels (LGICs). The nAChRs are members of cys-loop ligand-gated ion channels, which consist of a superfamily of pentameric channels with a cysteine-loop and four membrane spanning regions (TM1–TM4). This structure produces a mechanism that provides rapid synaptic transmission (Hille, 2001).

Although nAChRs are accepted to be a prototype of cationic cys-loop receptors (Karlin, 2002), both anionic and cationic examples of nAChRs exist in invertebrates (Chiarandini et al., 1967; Vulfius et al., 1967; Chemeris et al., 1982; van Nierop et al., 2005; Vulfius et al., 2005). The ion selectivity of the subunits can be predicted by analyzing their amino acid sequences. The second transmembrane domain (TM2) of anion-selective cys-loop receptors includes conserved Pro and

Ala regions (Galzi et al., 1992; Jensen et al., 2005). A nAChR without these conserved regions is predicted to be cation selective.

In addition to the studies of nAChR structure, there have also been many discoveries about the role of nAChRs on human physiology. An extensive list of neurophysiological functions of nAChRs has been cited in the literature, such as modulation of neurotransmitter release, neuronal integration, networking and cell excitability, which are important for processing of pain, sleep, arousal, fatigue, hunger and anxiety (Changeux and Edelstein, 2001; Hogg et al., 2003; Gotti and Clementi, 2004). Moreover, failures in the function of nAChRs in humans may lead to a wide range of diseases such as epilepsy, schizophrenia, myasthenia gravis, addiction and skin disorders (Lindstrom, 1997). These discoveries underline the importance of the nAChRs.

1.1.3 The history of the investigation of acetylcholine receptors

AChRs are one of the oldest and the most extensively studied class of receptors, which have been investigated in science for more than a century. H. H. Dale classified muscarinic and nicotinic types of cholinergic receptors in 1914, which is still a valid classification today. In the 1930s, Otto Loewi and H.H. Dale discovered that ACh is used as a neurotransmitter at the neuromuscular junction. Later, David Nachmansohn (1946) showed that the electrical organs of electric fish have high amounts of ACh.

The 1970s was one of the most luminous decade for the studies of ACh and nAChRs. In this decade, two animal species, *Torpedo californica* and the electric eel *Electrophorus electricus* were used as rich sources of nAChRs. One of the milestones in the studies of nAChRs was generating methodologies for the purification of the receptor. Michael Raftery and colleagues extracted the receptors from the cells of *Torpedo* electrical organ using detergents (Duguid and Raftery, 1973; Reed and Raftery, 1976). The venom of the banded krait snakes has a specific

type of toxin, α-bungarotoxin, which strongly binds to the nAChRs. The toxin can be extracted from the animal and labeled with iodine^{125} (Fertuck and Salpeter, 1974). Following the combination of the labeled toxin with the receptors, the receptors can be purified benefiting from the affinity chromatography methodology (Schmidt and Raftery, 1973). In 1979, nine articles characterizing AChRs were published in a single issue of a journal (ACS Journal Biochemistry, 1979, volume 18, issue 10) by Raftery's group. Four subunit types were described in the same issue. The pentameric structure of nAChRs was first described by Raftery (1980). The sequences of the four subunits were determined and found to be very similar to each other, which indicated that the subunits were derived from an ancestral gene. These discoveries were followed by the studies of the three-dimensional structure, ligand binding sites, and subtypes of the nAChRs. Determination of the three-dimensional structure of the receptors helped in the discovery of the receptor subunit composition.

The development of gene sequencing has been another milestone in the studies of ACh and its receptors. The first 54 amino acids of the *Torpedo* nAChR subunits were the first to be sequenced (Raftery, 1980). Having these sequences enabled scientists design primers, create oligonucleotide probes, and clone different receptors subunits. After that, families and super families of the nAChRs were discovered. The sequence information was a key factor for starting to analyze nAChRs at the molecular level.

1.1.4 Subunit definitions

The nAChRs are formed by five receptor subunits (Figure 1). Identified nAChR subunits have been named in the order of their identification. Previously, 17 types of nAChR subunits (10 α-subunits (α1–α10), four β subunits (β1–β4), and γ, δ, and ε subunits) were identified. Binding of one molecule of ACh to each of the α subunits produces conformational changes in the subunits,

and these changes cause the channel to open and transmit cations across the cell membrane.

The receptors generally incorporate a single type of α subunit and a single type of β subunit. However, expression experiments that were performed in *Xenopus* showed that two or three types of subunits could also come into play within a single receptor (Boorman et al., 2000). For instance, it was shown that α2, α3 or α4 will produce functional receptors only when they are teamed up with either β2 or β4. α7, α8 and α9. The subunits in this class can be functionally expressed as homomeric receptors without a β subunit in mammalian and *Xenopus* expression systems (Boulter et al., 1987; Deneris et al., 1988; Wada et al., 1988; Elgoyhen et al., 1994). Various combinations of these subunits form diverse pentameric nAChR receptor subtypes with different functionalities.

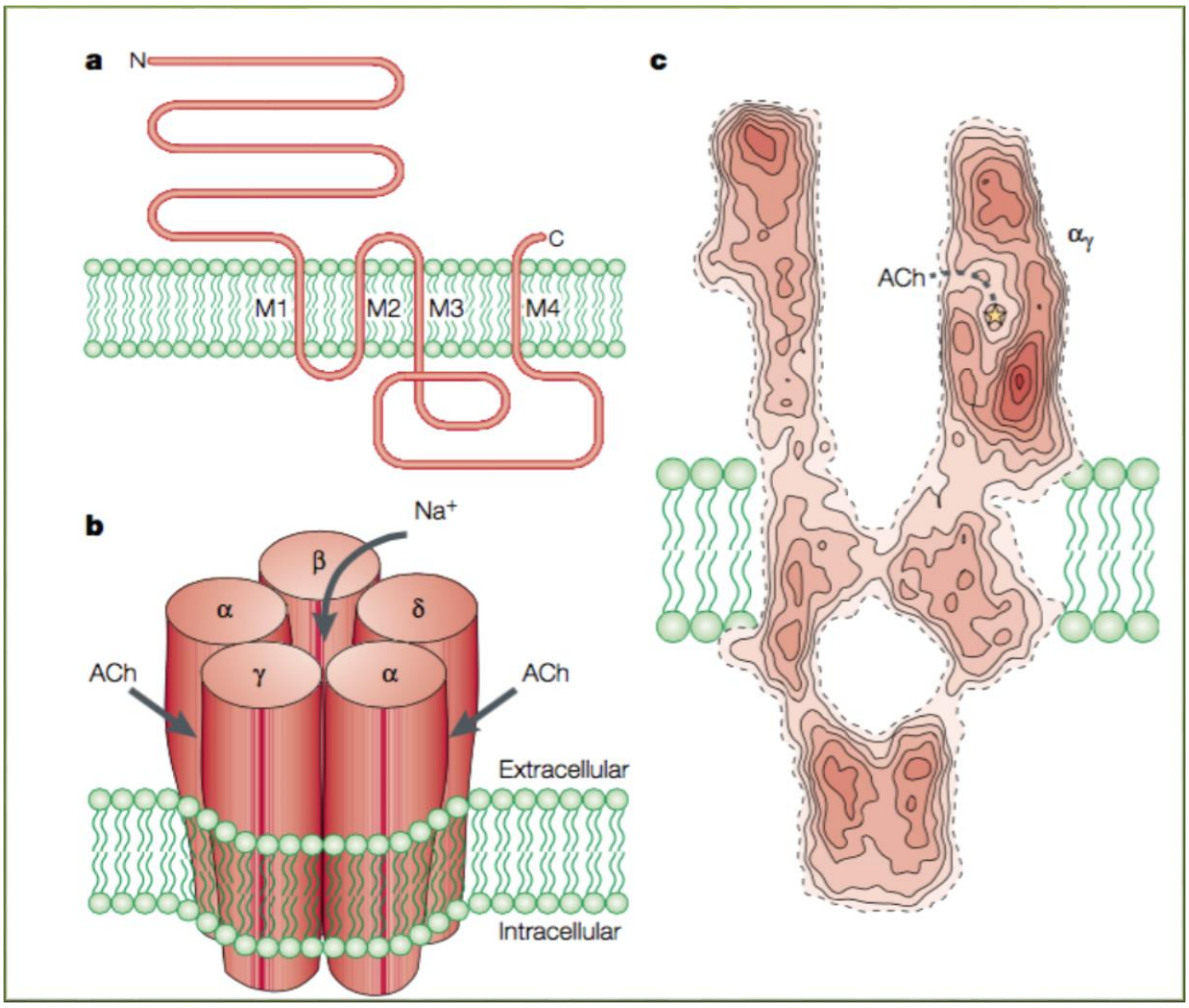

Figure 1 Structure of the nicotinic acetylcholine receptors (Karlin, 2002)

(a) The threading pattern of receptor subunits through the membrane. (b) A schematic representation of the quaternary structure, showing the arrangement of the subunits in the muscle-type receptor, the location of the two acetylcholine (ACh)-binding sites (between an α- and a γ-subunit, and an α- and a δ- subunit), and the axial cation-conducting channel. (c) A cross-section through the 4.6-Å structure of the receptor determined by electron microscopy of tubular crystals of Torpedo membrane embedded in ice.

1.1.5 nAChR in molluscs

Gardner and Kandel (1997) identified ACh and characterized its receptors in the buccal ganglia of *Aplysia californica* by measuring the sensitivity of the receptors to inhibitors, their kinetics to desensitization, and their conductance properties. They worked on four identified cholinergic interneurons in the buccal ganglia, and identified eight ipsilateral follower cells that they innervate. Their analyses resulted in the characterization of three types of potentials (Figure 2): excitatory postsynaptic potentials (EPSPs), inhibitory postsynaptic potentials (IPSPs), and biphasic E-IPSPs. Even though the receptors that produce EPSPs and E-IPSPs had some properties in common, they differed in their sensitivity to inhibitors. In addition, the conductance changes they produce differed in their reversal potential, duration, and functional consequences.

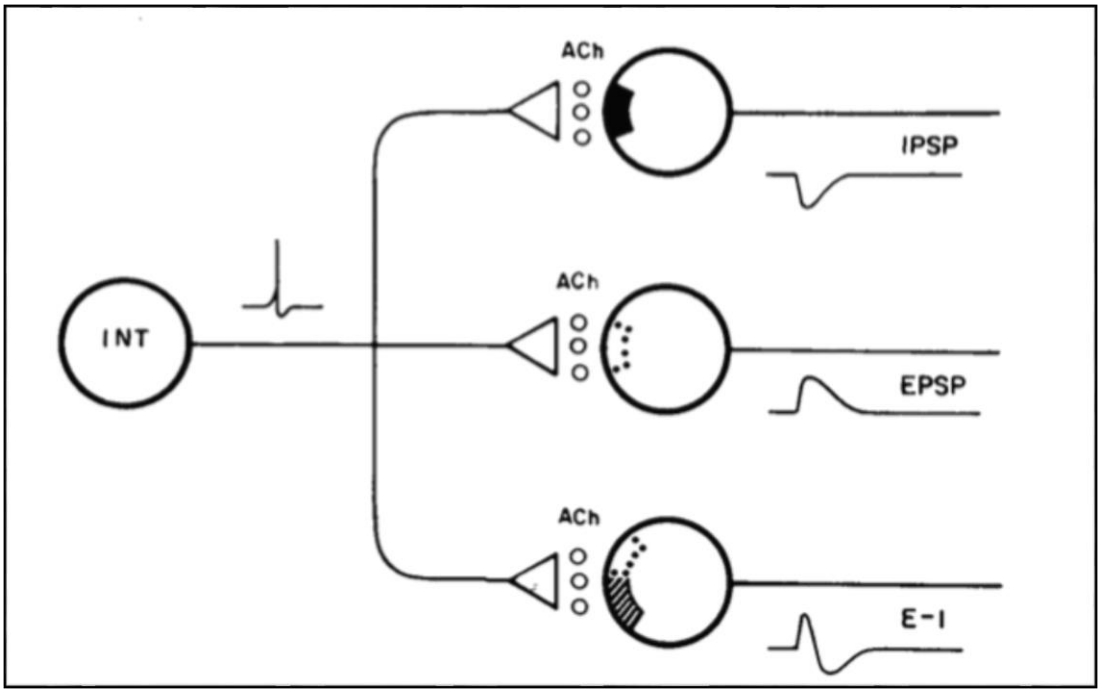

Figure 2 Gardner and Kandel's (1997) illustration of three types of cholinergic receptors on buccal ganglia cells

These potentials include IPSPs, EPSPs, and diphasic E-IPSPs. Dotted outlines indicated depolarizing receptors.

Even though Gardner and Kandel (1977) categorized different AChRs in *Aplysia*, they did not analyze the subunit composition in these receptors. The variety of receptor subunit combinations results in differences in the ion selectivity and functional characteristics of receptors. The subunit studies of molluscan nAChRs were hampered by the absence of molecular and sequence information, until the *Lymnaea* nAChRs were admirably investigated by van Nierop et al. (2005, 2006). Van Nierop et al. (2006) reported 12 nAChRs in the snail *Lymnaea* (LnAChR-A through LnAChR-L). Using these sequences, White et al. (2013) identified each of these subunits in *Aplysia* via BLAST searches. Additionally, they found nine more receptor subunits, which they called subunit J2, J3, K2, M, N, O, P, Q, and R. ApAChR J2 and J3 were similar to ApAChR-J1, and ApAChR K2 was similar to ApAChR-K1. These new receptor subunits, except ApAChR-N, were then also identified in *Lymnaea* central nervous system (CNS) transcriptome as LnAChRs (Sadamoto et al. 2012).

To identify cation and anion selective receptors, the presence of the conserved amino acid regions was investigated, including Pro and Ala that line the pore adjacent to the second transmembrane domain of anion-selective cys-loop receptors (Galzi et al. 1992; Jensen et al. 2005). Because of the absence of these conserved regions, 16 of the 21 subunits were identified as putative cation-selective subunits (Table 1). The presence of vicinal Cys192 and Cys193 (Torpedo numbering) (Kao et al. 1984; Sine, 2002) indicated potential α-receptors, whereas a lack of vicinal Cys indicated candidate β-receptors (Table 1).

Table 1 Predicted properties of molluscan nAChR subunits

	A	B	C	D	E	F	G	H	I	J	J2	J3	K	L	M	N	O	P	Q	R
Potential α receptors	x		x	x	x		x	x						x	x	x	x	x		x
Potential β receptors										x	x	x							x	
Potential anion selective receptors		x				x			x				x							
Potential cation selective receptors	x		x	x	x		x	x						x	x	x	x	x	x	x

Despite the studies on nAChR subunits in *Aplysia* and *Lymnaea*, subunits were not extensively studied in any other molluscan species. In this thesis research, I studied nAChR subunits in six nudipleuran species: *Flabellina, Hermissenda, Tritonia, Pleurobranchaea, Melibe* and *Dendronotus*.

The neural networks that control swimming behavior in these species are composed of homologous neurons (Sakurai et al. 2011). However, there are differences in synaptic wiring. It

was thought that different combinations of nAChR subunits and their differential might be responsible for the differences in the synaptic behavior. For example, anionic and cationic subunit composition may lead to differences in ion selectivity, which ultimately results in a difference in the sign of the synapse. Prior to testing such hypotheses, the nAChR subunit sequences have to be identified in these species. This thesis research identifies the sequence of nAChR subunits in the six species of Nudipleura, and establishes a basis for overarching goal of understanding the role of nAChR subunit composition in the inter-species differences of neural circuitries.

1.2 METHODS

1.2.1 Identification of nAChR subunits

Previously identified 20 nAChR subunits (Table 2) from *Lymnaea* and *Aplysia* were extracted from GenBank. BLAST searches were carried out on Linux command line through Georgia State University's high performance computing resources (http://ursa.research.gsu.edu/high-performance-computing/).

Using the previously created transcriptome database that is available in the laboratory of Dr. Paul S. Katz at Georgia State University, searchable BLAST databases were created for each of the six species using the 'makeblastdb' command, which is a BLAST+ feature (BLAST Command Line Applications User Manual [Internet]. Bethesda (MD): National Center for Biotechnology Information (US); 2008-. BLAST+ features. Available from: http://www.ncbi.nlm.nih.gov/books/NBK279668/). The command was run with ' -parse_seqids' option to enable retrieval of sequences based upon sequence identifiers. BLAST searches were carried out for each subunit against each of these databases using tblastn command with '-outfmt

7' option. To refine the results to the hits with E values (E values) smaller that e^{-80}, '-evalue 1e-80' option was used.

Table 2 Accession numbers of the query nAChR sequences that were extracted from web

Moluscan subunits	Genbank Accession	*Homo sapiens* subunits	Genbank Accession
ApAChR-A	KC417388	CHRNα1	NM_001039523
LnAChR-B	DQ167345	CHRNα2	NM_000742
ApAChR-C	KC411667	CHRNα3	NM_000743
ApAChR-D	KC411668	CHRNα4	NM_000744
ApAChR-E	KC411669	CHRNα5	NM_000745
LnAChR-F	DQ16734	CHRNα6	NM_004198
ApAChR-G	KC411660	CHRNα7	NM_000746
ApAChR-H	KC411661	CHRNα9	NM_017581
LnAChR-I	DQ167352	CHRNα10	NM_020402
LnAChR-J	DQ167354	CHRNβ1	NM_000747
ApAChR-J2	KC417389	CHRNβ2	NM_000748
ApAChR-J3	KC417390	CHRNβ3	NM_000749
LnAChR-K	DQ167353	CHRNβ4	NM_000750
ApAChR-L	KC618637	CHRNδ	NM_000751
ApAChR-M	KC618636	CHRNδ	NM_005199
ApAChR-N	KC411662	CHRNε	NM_000080
ApAChR-O	KC411663		
ApAChR-P	KC411664		
ApAChR-Q	KC411665		
ApAChR- R	KC411666		
GABA-A receptor α subunit	AF322878		

After BLAST, the receptors subunits were identified in Nudipleura based on the success of BLAST hits, which were determined by looking at E values. The fasta files for selected sequences were extracted from databases through 'blastdbcmd' command. Nucleic acid sequences were saved into a text file, and translated into protein sequences using the 'transeq' command of EMBOSS (http://emboss.sourceforge.net). The longest open reading frames (ORF) were selected manually. Additional information is provided in the appendix part.

1.2.2 Identification of orphan nAChR subunits

Putative novel nAChRs were predicted based on E values, with an ortholog-based approach. After *Aplysia* subunit sequences were blasted against Nudipleura transcriptomes, an iterative approach was taken. First, all results for 20 subunits in six nudipleuran species with E values smaller than e^{-80} were printed on command line screen (Figure 3A) and then were copied into a modifiable text file.

Generally, the top result pointed out a gene that has a zero-E-value, indicating a significant BLAST hit and there was only a single component ID that has zero-E-value (Figure 3B). For such cases, this component ID was thought to be the ortholog of the query gene in the Nudipleura species that was investigated (Figure 3C). Therefore, the ID was renamed to the corresponding subunit name. This renaming affected all results that were in the text file. For instance, after "comp74013_c7" (Figure 3C) was renamed as "Pleurobranchaea Sub A". Many "comp74013_c7" that appeared in the BLAST results of all 20 subunits were actually replaced; because some groups of subunits were closely related to each other, they gave significant BLAST hits for each other.

The process was repeated for all subunits in all species, and all top results with zero-E-values were renamed in all BLAST results. After that, most of the component IDs were found to be changed. The IDs that were not changed (as labeled with question mark in Figure 3D) were thought to be orphan nAChR subunits.

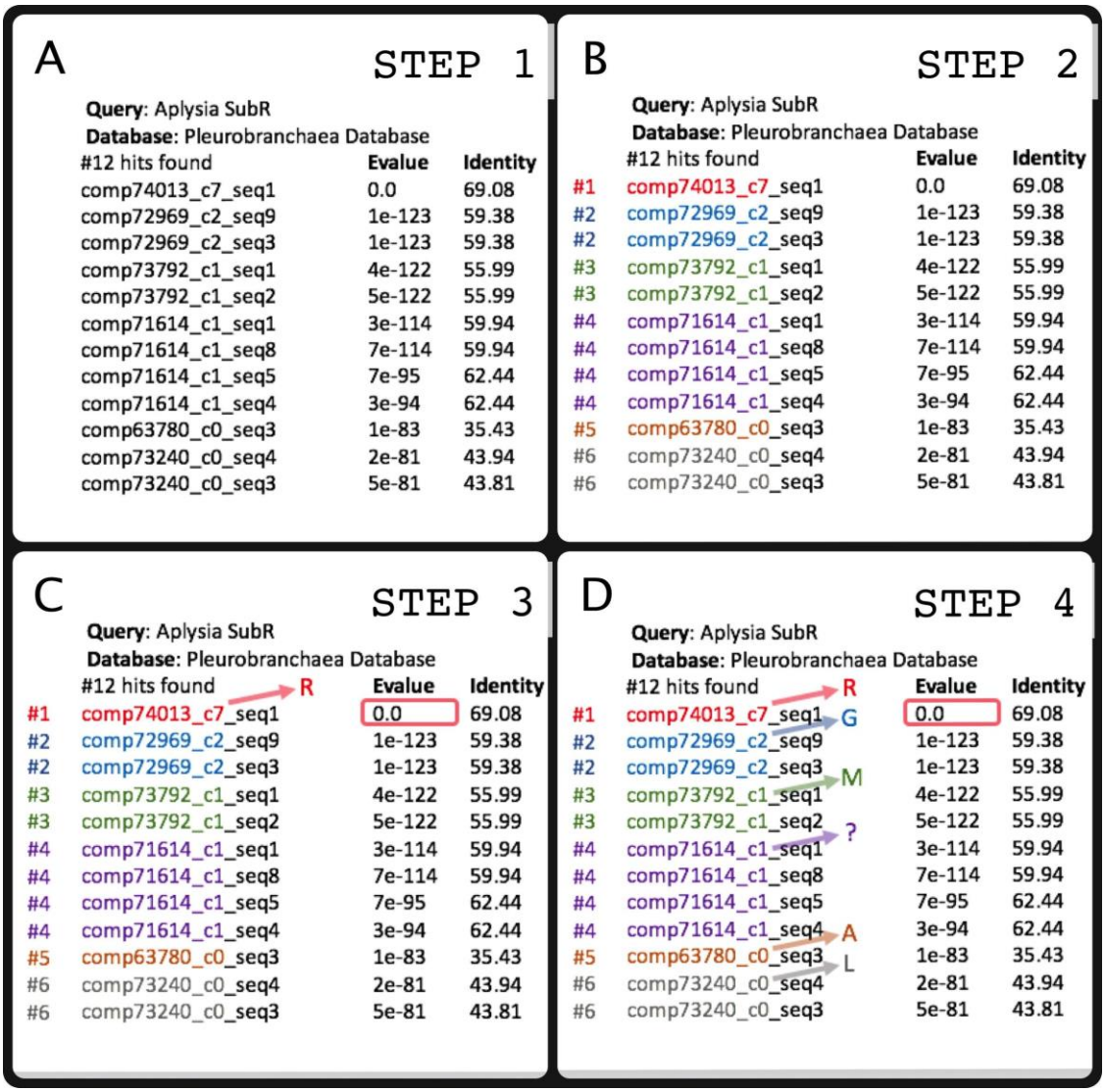

Figure 3 Illustration of the method that is used for the identification of the novel subunits

1.2.3 De-orphanizing orphan nAChR subunits

To de-orphanize the identified orphan subunit sequences, hierarchical clustering was performed in R using all identified subunit sequences and all orphan subunit sequences and then the phylogeny was plotted. If an orphan sequence clustered with a unique type of previously identified subunit sequences, the sequence was thought to be of that subunit type. If several orphan receptors create a cluster that does not include a previously identified type of subunit, it was predicted as a novel nAChR subunit and assigned to a new subunit name.

In order to create phylogenetic trees, all protein sequences were saved into a single file in fasta format. Alignments were performed through CLUSTALW alignment in MEGA (Kumar, 2016) using BLOcks SUbstitution Matrix (BLOSUM). After the alignment was complete, it was exported as a fasta file then uploaded into R (Team, 2013) using ‘read.alignment’ function in the Bioconductor’s ‘SeqinR’ package (Charif and Lobry, 2007). A similarity distance matrix was calculated in R using ‘dist.alignment' function. NaN values were replaced with 0.8 in the matrix. Then, hierarchical clustering was performed using ‘hclust’ function in R, with ‘Ward.D2’ agglomeration method, which aims at finding compact and spherical clusters. The "Ward.D2" option implemented Ward's (1963) clustering criterion (Murtagh and Legendre 2014), where the dissimilarities were squared before cluster updating.

The resulting object was converted into a tree as a ‘phylo’ class through ‘as.phylo’ function available in the package ‘ape’ (Paradis et al., 2004). Phylogenetic tree was created using the generic ‘plot’ function in R, and the type of the plot was set as ‘fan’. Different clades were colored differently by clustering object with ‘cutree’ function.

1.2.4 Bootstrap analysis in R

The multiple sequence alignment that was created in MEGA was read into R using 'read.phyDat' function in the Phangorn package. A distance matrix was created via list.logDet function, then 'NJ' function was used to create neighbor-joining clustering. Maximum Parsimony analysis was performed through Phangorn package, using a bootstrap value of 1000. R codes are provided in the Appendix.

1.2.5 Maximum Likelihood and timetree analyses in MEGA

Maximum Likelihood and timetree analyses were conducted in MEGA7 (Kumar, 2015). The evolutionary history was inferred by using the Maximum Likelihood method based on the Poisson correction model (Zuckerkandl, 1965). Initial tree(s) for the heuristic search were obtained automatically by applying Neighbor-Join and BioNJ algorithms to a matrix of pairwise distances estimated using a JTT model, and then selecting the topology with superior log likelihood value. The tree is drawn to scale, with branch lengths measured in the number of substitutions per site. All positions with less than 95% site coverage were eliminated. That is, fewer than 5% alignment gaps, missing data, and ambiguous bases were allowed at any position.

1.2.6 Calculation of RSEM Expression Values

Before RSEM values are determined, the best transcript was carefully selected among several possible candidate transcripts to be used for RSEM calculation. Typically, there were 1-5 transcript hits with the same component ID in a BLAST result. They generally had the same E value and percentage identity. In order to select the transcript to be used for RSEM calculation, IsoPct values (percentage of expression for given transcript compared with all expression from that Trinity component) were analyzed. Generally, only one transcript had significant IsoPct value among the best candidates. The hit with the greatest IsoPct value was used for RSEM

calculation. In a few cases, there were more than one hits with similar IsoPct values. However, the RSEM values of those hits were also close to each other, and the selection did not much make a difference.

1.3 RESULTS

1.3.1 Identification of receptor subunits based on E Values

The receptors subunits (A-R) were identified in the six nudipleuran species based on the success of BLAST hits. The percentage identities and E Values of the BLAST hits are provided in Table 3. The range of E values is indicated in different highlighting colors. In general, BLAST results gave a unique component ID with a zero-E-value, which helped easily recognizing and identifying the sequence of interest. Non-zero-E-Values were observed for subunit H, O, P and Q. Although the E values of the best BLAST hits were not zero, they were very low (generally lower than e^{-150}), and there was a unique component ID that has a very low E value. Therefore, these subunits were also identified confidently.

The receptor subunit N did not give any significant BLAST hit for any of the six species. The same receptor subunit was also the only non-identifiable subunit in *Lymnaea* CNS among 21 nAChR subunits (Sadamoto et al. 2012). The only significant BLAST hit for receptor subunit P was observed in *Melibe*, among the six species.

Table 3 Percentage identity values of the top BLAST hits

Highlighting colors are based on E values (Eval). (Green: EVal=0; Blue: e^{-180}<EVal<l e^{-150}; Yellow: e^{-150}<EVal<e^{-120}; White: e^{-120}<EVal<e^{-100} or N/A.)

	Mel	Den	Fla	Her	Tri	Ple	Avg	SD
A	78	79	78	78	79	79	78.50	0.55
B	72	70	71	70	73	69	70.83	1.47
C	79	80	78	78	79	84	79.67	2.25
D	70	N/A	N/A	N/A	71	N/A	70.50	0.71
E	81	81	85	82	85	83	82.83	1.83
F	73	74	72	70	73	74	72.67	1.51
G	85	83	82	82	76	87	82.50	3.73
H	55	52	56	54	57	58	55.33	2.16
I	72	73	72	70	72	73	72.00	1.10
J	73	85	73	73	74	77	75.83	4.75
J2	N/A	58	59	59	59	53	57.60	2.61
J3	N/A	N/A	N/A	N/A	N/A	N/A	N/A	N/A
K	74	45	77	72	75	50	65.50	14.12
L	77	75	80	76	78	85	78.50	3.62
M	69	67	66	68	*89*	*78*	72.83	9.02
N	N/A	N/A	N/A	N/A	N/A	N/A	N/A	N/A
O	67	65	68	70	71	66	67.83	2.32
P	62	N/A	N/A	N/A	N/A	N/A	62.00	N/A
Q	61	69	64	64	69	68	65.83	3.31
R	67	58	68	68	68	69	66.33	4.13

1.3.2 De-orphanizing orphan nAChR subunits

After component IDs were renamed as explained in the Methods, the remaining component IDs in the BLAST results were renamed as orphan AChRs as shown in the first two columns of Table 4. This process yielded 33 orphan receptor subunits; four in *Tritonia*, six in *Pleurobranchaea*, seven in *Melibe*, six in *Hermissenda*, four in *Flabellina*, and six in *Dendronotus*. After that, hierarchical clustering was performed and plotted (Figure 4) for all identified nAChRs, along with all orphan nAChRs. Previously identified *Aplysia* and *Lymnaea* nAChR subunits were also included in the tree. Some orphan subunits clustered together, having a unique sequence from each species in the cluster. In total, there were four such clusters, which were predicted to be novel nAChR receptor subunits. These subunits were named as subunit K2, L2, S and T (Figure 4). Some of the remaining orphans were predicted to be the missing members of previously identified receptor subunit types. Subunit P, D and K in *Pleurobranchaea*, R and N in *Dendronotus*, J2 in *Melibe* were identified. Furthermore, an additional subunit that is close to subunit R was detected for *Dendronotus*, and indicated as R2 in the figure. Similarly, D2 in *Pleurobranchaea*, D3 in *Melibe*, J4 in *Pleurobranchaea* and *Hermissenda* were predicted. This procedure of de-orphanization is outlined in Table 4. In total, 123 subunits were identified and named as indicated in Table 5. After annotation is completed, hierarchical clustering was re-plotted and provided in Figure 5. Subunits that are predicted to be anion selective (Table 1) were clustered together as indicated by the minus sign at the center of the tree.

Table 4 Identification of orphan nAChR subunits and de-orphanizing them

comp69295_c1_seq2		OrphanTriAChR1		T_Tri
comp69523_c1_seq5	→	OrphanTriAChR2	→	K2_Tri
comp62518_c0_seq2		OrphanTriAChR3		S_Tri
comp63825_c0_seq1		OrphanTriAChR4		L2_Tri
comp71614_c1_seq1		OrphanPleAChR1		S_Ple
comp103363_c0_seq1		OrphanPleAChR2		D_Ple
comp156886_c0_seq1	→	OrphanPleAChR3	→	D2_Ple
comp66868_c2_seq1		OrphanPleAChR4		K_Ple
comp70685_c0_seq1		OrphanPleAChR5		L2_Ple
comp57491_c2_seq1		OrphanPleAChR6		P_Ple
comp74388_c2_seq1		OrphanMelAChR1		T_Mel
comp62509_c0_seq2		OrphanMelAChR2		K2_Mel
comp66522_c2_seq3		OrphanMelAChR3		S_Mel
comp72328_c1_seq2	→	OrphanMelAChR4	→	L2_Mel
comp63165_c1_seq1		OrphanMelAChR5		J3_Mel
comp76107_c1_seq1		OrphanMelAChR6		J2_Mel
comp76107_c0_seq5		OrphanMelAChR7		
comp85084_c1_seq2		OrphanHerAChR1		T_Her
comp85398_c0_seq3		OrphanHerAChR2		K2_Her
comp79379_c0_seq1	→	OrphanHerAChR3	→	K3_Her
comp78981_c2_seq3		OrphanHerAChR4		S_Her
comp82679_c1_seq4		OrphanHerAChR5		L2_Her
comp86880_c0_seq9		OrphanHerAChR6		J4_Her
comp68440_c0_seq8		OrphanFlaAChR1		T_Fla
comp61409_c0_seq1		OrphanFlaAChR2		S_Fla
comp67700_c1_seq1	→	OrphanFlaAChR3	→	K2_Fla
comp48424_c0_seq1		OrphanFlaAChR4		J4_Fla
comp78206_c3_seq1		OrphanDenAChR1		K2_Den
comp73998_c0_seq2		OrphanDenAChR2		S_Den
comp76205_c3_seq1	→	OrphanDenAChR3	→	R2_Den
comp74858_c2_seq1		OrphanDenAChR4		L2_Den
comp75516_c1_seq4		OrphanDenAChR5		P_Den
comp76205_c1_seq1		OrphanDenAChR6		R_Den

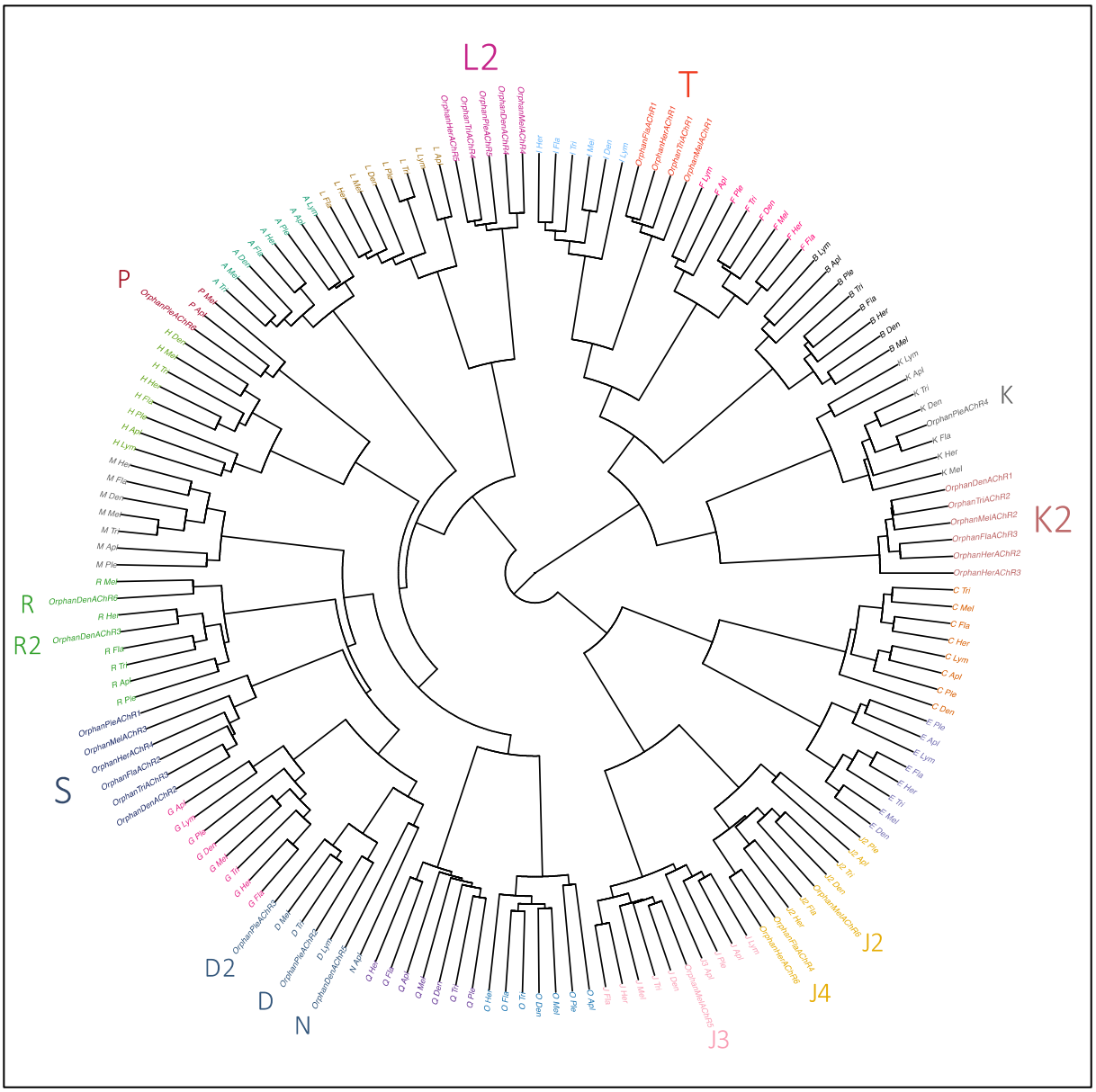

Figure 4 De-orphanizing orphan nAChRs

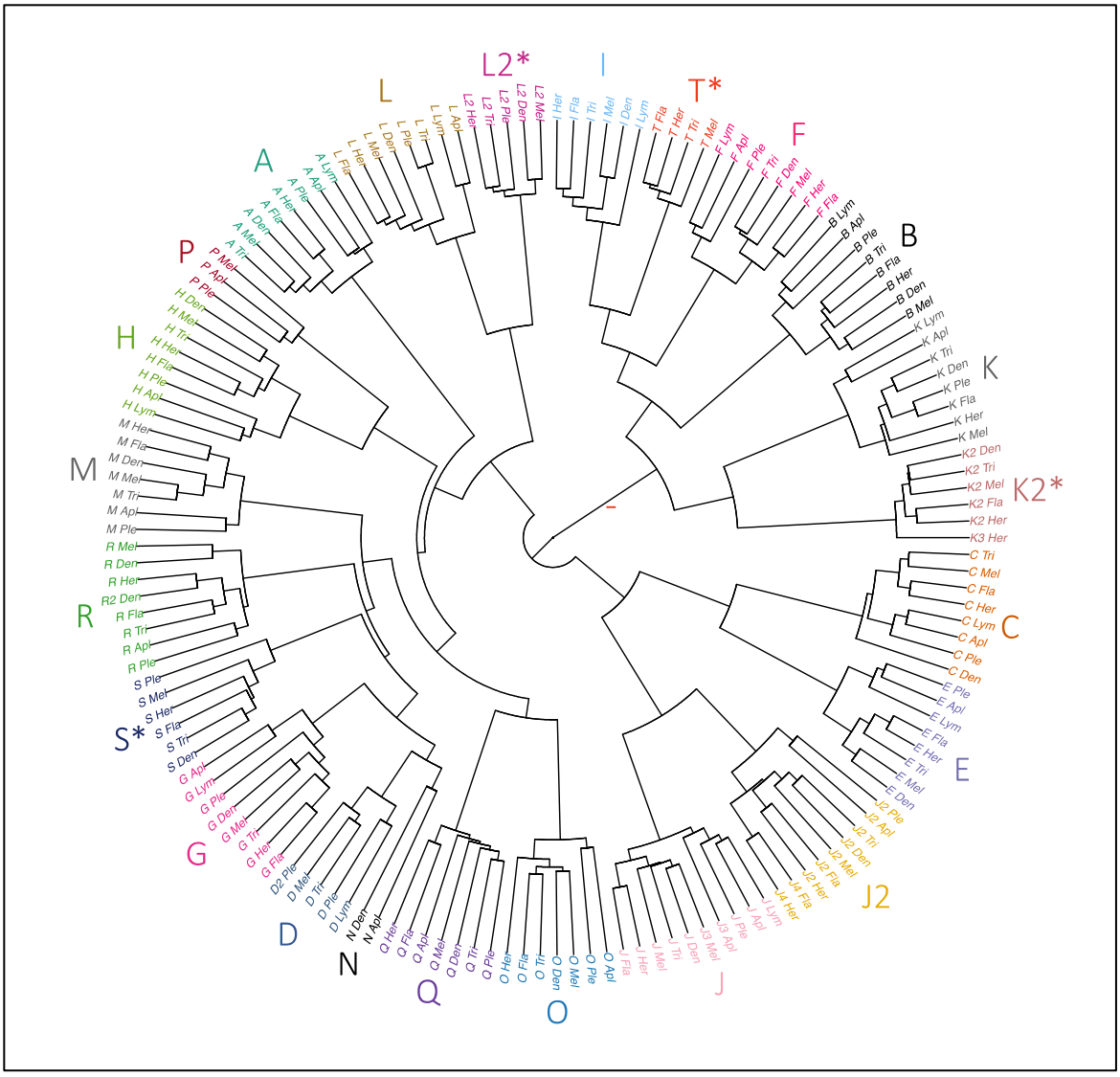

Figure 5 A plot of hierarchical clustering of the identified nAChR subunits

The four novel putative subunits are indicated with star. A minus sign is placed at the center of the tree to indicate the clade of putative anion selective subunits.

Table 5 Nomenclature of the identified nAChR subunits

	Dendronotus	*Melibe*	*Hermissenda*	*Flabellina*	*Pleurobranchaea*	*Tritonia*
Subunit A	AChR-A-Den	AChR-A-Mel	AChR-A-Her	AChR-A-Fla	AChR-A-Ple	AChR-A-Tri
Subunit B	AChR-B-Den	AChR-B-Mel	AChR-B-Her	AChR-B-Fla	AChR-B-Ple	AChR-B-Tri
Subunit C	AChR-C-Den	AChR-C-Mel	AChR-C-Her	AChR-C-Fla	AChR-C-Ple	AChR-C-Tri
Subunit D		AChR-D-Mel			AChR-D-Ple	AChR-D-Tri
Subunit E	AChR-E-Den	AChR-E-Mel	AChR-E-Her	AChR-E-Fla	AChR-E-Ple	AChR-E-Tri
Subunit F	AChR-F-Den	AChR-F-Mel	AChR-F-Her	AChR-F-Fla	AChR-F-Ple	AChR-F-Tri
Subunit G	AChR-G-Den	AChR-G-Mel	AChR-G-Her	AChR-G-Fla	AChR-G-Ple	AChR-G-Tri
Subunit H	AChR-H-Den	AChR-H-Mel	AChR-H-Her	AChR-H-Fla	AChR-H-Ple	AChR-H-Tri
Subunit I	AChR-I-Den	AChR-I-Mel	AChR-I-Her	AChR-I-Fla	AChR-I-Ple	AChR-I-Tri
Subunit J	AChR-J-Den	AChR-J-Mel	AChR-J-Her	AChR-J-Fla	AChR-J-Ple	AChR-J-Tri
Subunit J2	AChR-J2-Den	AChR-J2-Mel	AChR- J2-Her	AChR- J2-Fla	AChR- J2-Ple	AChR- J2-Tri
Subunit K	AChR-K-Den	AChR-K-Mel	AChR-K-Her	AChR-K-Fla	AChR-K-Ple	AChR-K-Tri
Subunit K2	AChR-K2-Den	AChR- K2-Mel	AChR- K2-Her	AChR- K2-Fla	AChR-K2-Ple	AChR- K2-Tri
Subunit L	AChR-L-Den	AChR-L-Mel	AChR-L-Her	AChR-L-Fla	AChR-L-Ple	AChR-L-Tri
Subunit L2	AChR-L2-Den	AChR- L2-Mel	AChR- L2-Her		AChR- L2-Ple	AChR- L2-Tri
Subunit M	AChR-M-Den	AChR-M-Mel	AChR-M-Her	AChR-M-Fla	AChR-M-Ple	AChR-M-Tri
Subunit O	AChR-O-Den	AChR-O-Mel	AChR-O-Her	AChR-O-Fla	AChR-O-Ple	AChR-O-Tri
Subunit P		AChR-P-Mel			AChR-P-Ple	AChR-P-Tri
Subunit Q	AChR-Q-Den	AChR-Q-Mel	AChR-Q-Her	AChR-Q-Fla	AChR-Q-Ple	AChR-Q-Tri
Subunit R	AChR-R-Den	AChR-R-Mel	AChR-R-Her	AChR-R-Fla	AChR-R-Ple	AChR-R-Tri
Subunit S	AChR-S-Den	AChR-S-Mel	AChR-S-Her	AChR-S-Fla	AChR-S-Ple	AChR-S-Tri
Subunit T		AChR-T-Mel	AChR-T-Her	AChR-T-Fla		AChR-T-Tri

1.3.3 Phylogenetic analysis of nAChR subunits

A phylogenetic analysis was performed on the identified nAChR subunits using the Maximum Likelihood (ML) method (Figure 6). In addition, a bootstrap analysis was carried out through Maximum Parsimony (MP) methodology. The 16 human nicotinic receptor subunit sequences were also included in the ML analysis. *Aplysia* GABA-A subunit was used as an out-group to root the tree.

In the ML (Figure 6), each type of subunit clustered within each other. The putative anion selective subunits (B, F, I, K, K2, T) formed a separate clade on the tree. Among the putative cation selective subunits, the subunits G, D, M, R, S clustered closely with each other. These subunits also had very similar BLAST results. Subunit A is closely clustered with human nAChR subunit α7, whereas none of the remaining human subunits is clustered with the molluscan subunits that close. In addition, Subunit E and C were closer to the human subunits when compared to the other molluscan subunits.

In the MP tree, the upper part consists of the putative anion-selective subunits (B, F, I, K, K2, T) and the lower part consists of the putative cation-selective subunits. Subunit H, P, O and Q laid at the bottom, having an ancestral position to anion and cation selective subunits. The ancestral position of subunits H, P, and O are confirmed by ML tree. In Figure 8 provides a schematic drawing showing a possible scenario about the evolution of nAChR subunits. Subunit Q is not included in this figure because its position in ML analysis was not supported by MP methodology.

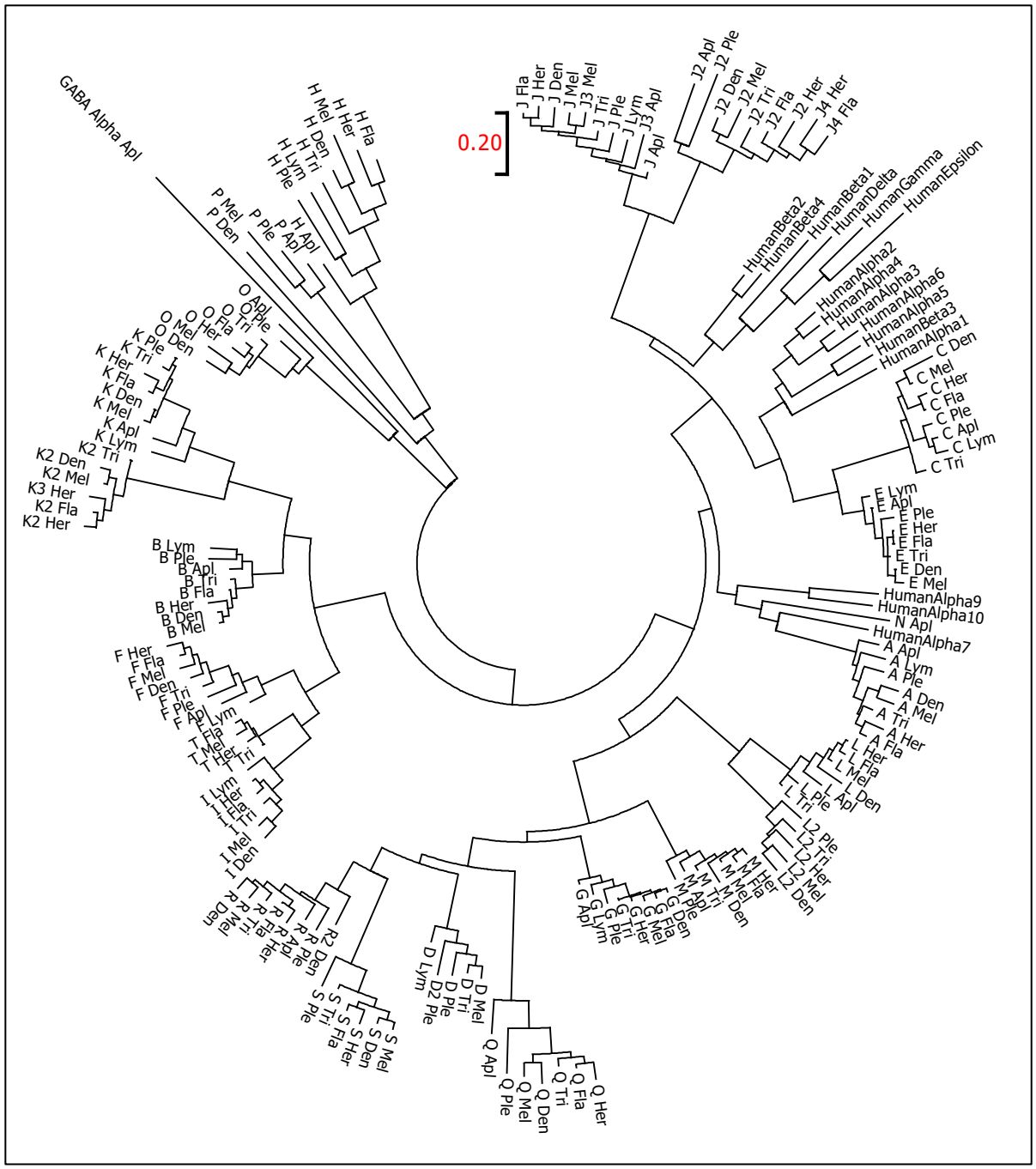

Figure 6 Molecular phylogenetic analysis of the identified nAChR subunits by Maximum Likelihood method

An orphan receptor that was previously predicted as Subunit N in *Dendronotus* was clustered together with the subunit P sequences, therefore, it was renamed as Subunit P in this tree. However, this sequence was not annotated and included in the nomenclature table (Table 5) because of the conflict.

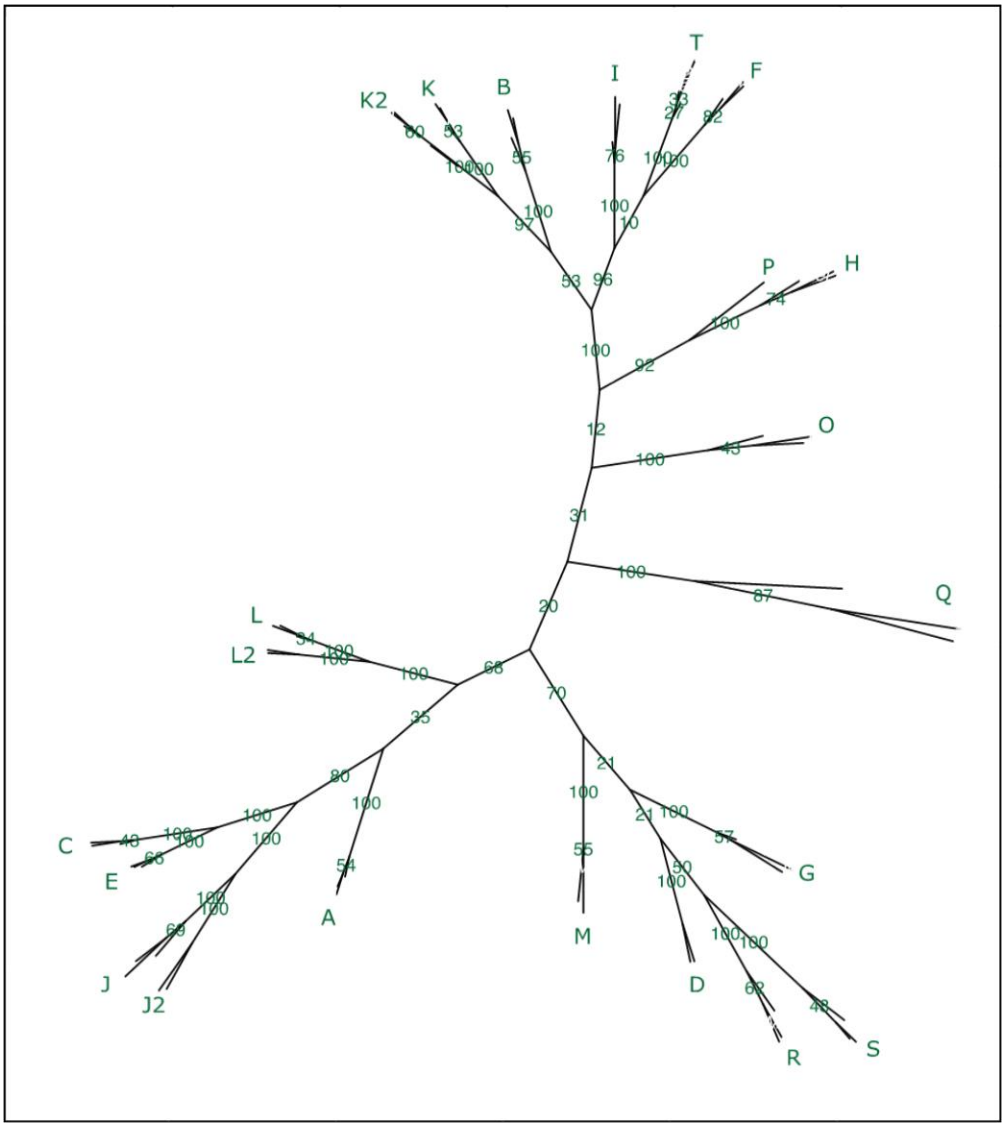

Figure 7 Unrooted tree of nAChR subunits of three species using Maximum Parsimony method

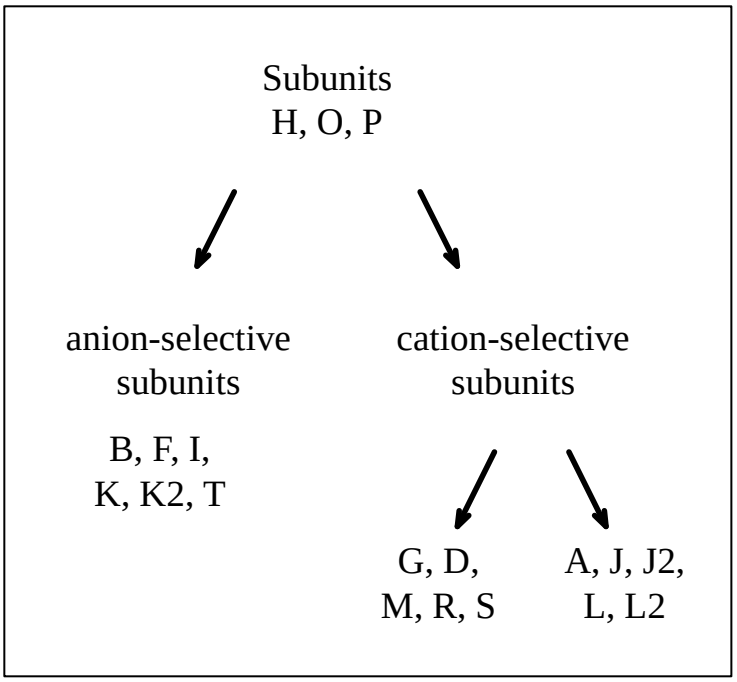

Figure 8 A possible scenario about the evolution of molluscan nAChR subunits

1.3.4 Expression values

RSEM expression values for the identified nAChR subunits were determined and potted (Figure 9, 10, and 11). One-way ANOVA analysis between subunits showed that the mean expression values of different subunits were significantly [$F(17,90) = 3.77$, $p = 0.013$] different from each other. Subunit G was highly expressed in all species, whereas the expression of S, E, K and I were low in general. In addition, between-species variability of expression values was examined further. Expression levels of subunits H, J, A, and B were highly variable within all species, whereas the variability for subunits E, S, L and J2 was low.

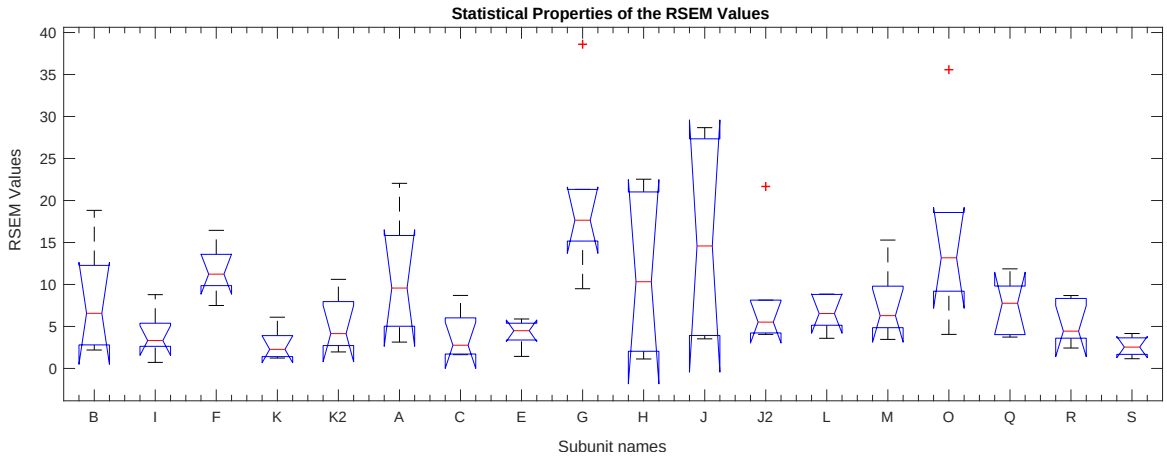

Figure 9 The boxplot of RSEM expression values

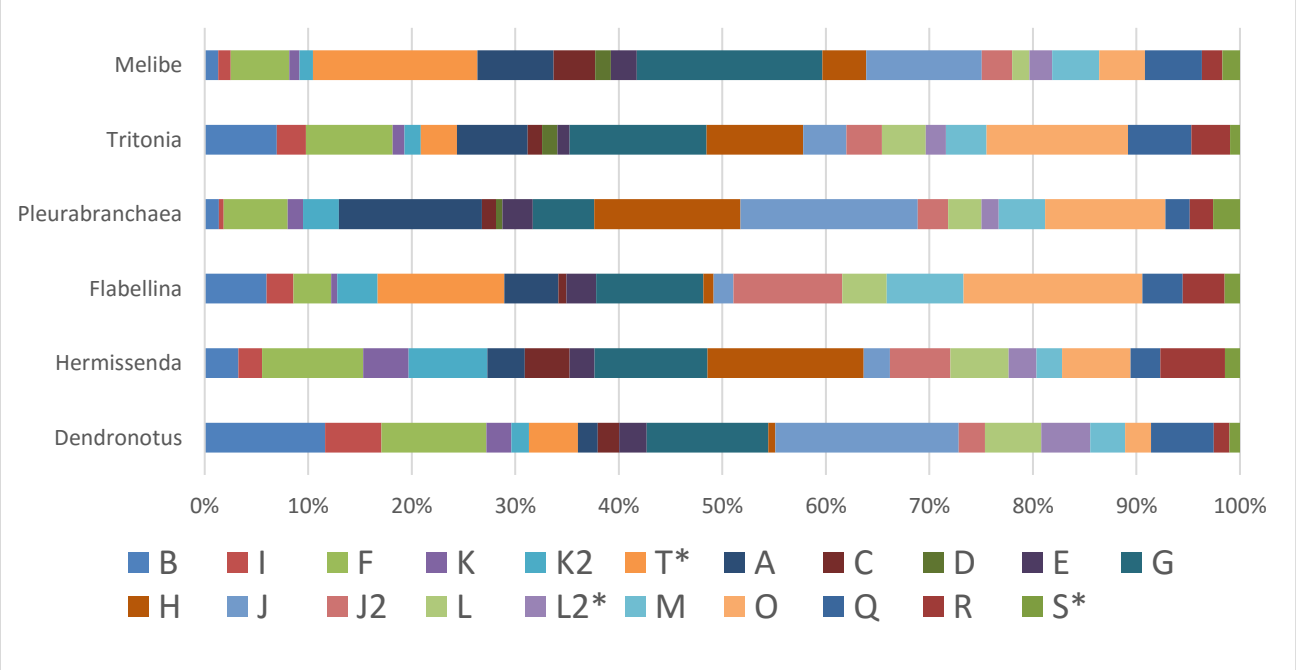

Figure 10 RSEM expression values are plotted in 100% stacked bar

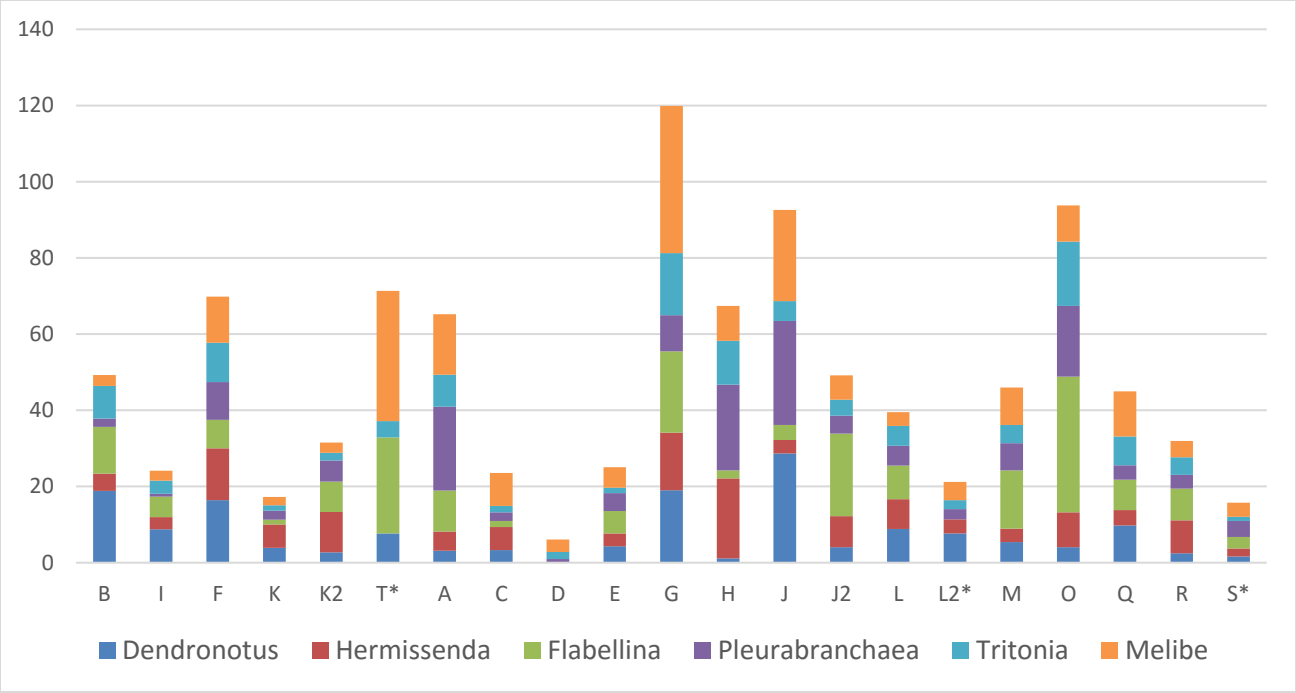

Figure 11 RSEM expression values plotted in stacked bar

1.4 DISCUSSION

In this part of thesis study, twenty types of molluscan nAChR subunits were identified in six nudipleuran species. In addition, four novel types of putative nAChR subunits were discovered with an ortholog-based approach. The identified sequences were analyzed to discover their evolutionary relations and gene expression levels.

1.4.1 Identification of receptor subunits and de-orphanizing orphan nAChRs

The receptors subunits (A-R) were identified in the six species based on the success of BLAST hits, which were determined by looking at the E values in BLAST results. The E value indicates the validity of the match: the smaller the E value, the less likely the match is by chance. In other words, the smaller the E values, the more likely the match represents real similarity (McGinnis, 2004). The E value scales with the size of the database. When a database in which most of the

sequences are not of interest, the false-positive rate becomes higher. In this analysis, each species had an individual database, rather than having a common database for each species. Therefore, the E value, in our case, is a very appropriate and reliable tool for identification of the sequences.

After 20 subunits were identified, 33 orphan nAChRs were detected in the BLAST results. Then, another phylogenetic tree was created to de-orphanize them. These analyses yielded four putative novel nAChR subunits. The prediction was supported by an orthologue and phylogeny-based approach, where clustering of each type of novel subunits from the six nudipleurans validated the prediction of novel subunits. Therefore, studying gene families in a quantity of species could be much more advantageous than studying them in a single species when discovering novel genes. This protocol serves as a novel methodology for identification of the orphan genes in transcriptomes of the species that belong to same phylum.

The receptor subunit N did not give any significant BLAST hit for any of the six species. The same receptor subunit was also the only non-identifiable subunit in *Lymnaea* CNS among 21 nAChR subunits (Sadamoto et al. 2012). The only significant BLAST hit for receptor subunit P was observed in *Melibe*, among the six species. White et al. (2014) also encountered problems with the identification of subunit P because it was too short. However, subunit P was later identified in *Pleurobranchaea* and *Tritonia* during ML analysis.

1.4.2 Nomenclature of the identified sequences

In total, 123 subunits were identified and named as in Table 5. The receptors were named as AChR rather than nAChR to continue the convention in the studies of White et al. (2014). When naming the four novel putative nAChR subunits, similarities between subunits were taken into consideration. Subunit K2 was named so because it was very close to subunit K both in BLAST

results and phylogeny. Likewise, subunit L2 was also named based on its similarity with subunit L. On the other hand, subunit T was closest to either subunit I or subunit F, depending on species, in BLAST results. Therefore, rather than saying I2 or F2, this new clade was named with a new letter: T. Subunit S was also a novel nAChR that is named in this thesis research.

1.4.3 Phylogeny

Both in ML and MP analyses, anion and cation selective subunits are clustered within itself. Furthermore, subunits H, P, and O are predicted to be ancestral to anion and cation selective subunits (Figure 6 and 7) because of their position in ML and MP trees. A similar analysis and conclusion is also true for human nAChR subunit sequences, where α7, α8 and α9 were predicted to be ancestral to other types of human nAChR subunits because of their position in the phylogenetic tree (Tsunoyama and Gojobori, 1998)

An unrooted tree with bootstrap analysis was created (Figure 7) using the subunit sequences of *Melibe*, *Dendronotus* and *Hermissenda*. Putative anion selective subunits (Subunits B, F, I, K, K2, T) were clustered together at the upper side of the tree, and the separation of this clade had a bootstrap value of 100. This suggests that two of the four newly identified subunits, subunit K2 and T, are most likely anion selective subunits. The cluster of subunit C and E, the cluster of subunits L and L2, as well as the cluster of subunits J and J2 also had bootstrap values of 100 on top of their clades, showing strong and reliable relationship within each other. Subunits O, Q, P and H were found to be far from the rest of the subunits in the tree. This pattern agrees with the BLAST results in Table 3, where they were the only subunits that were highlighted with blue because of an E value between e^{-150} and e^{-180}. The reason why they did not have a zero-E-value was because their separate positioning in their evolution, and not because of an experimental bias in the analysis.

1.4.4 RSEM Expression Values

The expression levels were predicted based on RSEM methodology. One-way ANOVA showed that the mean expression values of different subunits were found significantly different from each other. The RSEM values were assessed with one-way ANOVA between subunits and the mean subunit expression values were found significantly different from each other. Subunit G had the highest expression levels, and this was consistent across all of the six species. However, when Nierop et al. (2005) examined expression of subunits in *Lymnaea*, and found that subunit G is expressed in a very low extent in *Lymnaea*. The same study also found that subunit F and H had the highest expression values among 12 nAChR subunits (subunits A-L). On the contrary, subunit F had one of the lowest expression values in our analysis. However, the abundant expression of subunit H was consistent. White et al. (2014) also analyzed the expression levels of 16 nAChR subunits in *Aplysia* and found that subunit Q had the highest expression, contrary to our results. These comparisons show that subunit expression levels may be highly variant among species.

1.4.5 Conclusion and Future Perspectives

This chapter presented a comprehensive analysis of nAChR subunits in nudipleuran molluscs. Twenty types of nAChR subunits that were previously identified in gastropod molluscs were identified in six Nudipleura. Four novel nAChR subunits were predicted with an ortholog-based approach. The evolutionary relations and gene expression levels were determined and analyzed. These analyses are important for understanding the variety, evolution and function of nAChR subunits in molluscan species.

In the future, analyzing the subunit expression in single identified neurons rather than the whole CNS would help to understand the role of these subunits in neural networks. In this regard, this

study is aimed to be followed up by investigation of the identified nudipleuran subunits in single neurons that are included in the swim central pattern generator (CPG) of these nudipleurans. The homologs of CPG neurons have already been identified across several nudipleurans, and synaptic differences have been well characterized (Lillvis, 2012; Newcomb, 2012; Sakurai, 2013). As of now, differences in receptor subunit composition and expression can give an explanation for the differences in the CPG activity. Single cell qPCR and single cell RNA-Sequencing experiments can serve as appropriate methodologies for such analyses. Thereby, these analyses can contribute to our understanding of how variety in receptor subunit composition regulates electrical activity in the neural networks of these species. Furthermore, the functionality of the subunits could be determined by calculating the ratio of synonymous and non-synonymous substitutions to propose better evolutionary hypotheses.

2 CHAPTER 2: CHOLINERGIC NEURONS

2.1 INTRODUCTION

2.1.1 Acetylcholine in the nervous system

Acetylcholine (ACh) is one of the most abundant neurotransmitters in the nervous system throughout animals. (Venter et al., 1988). It has a diverse range of uses in different organisms, from unicellular organisms and plants to humans. Plants use ACh in defense mechanisms and for development and control of membrane permeability. Bacteria secrete it and use it as a carbon source (Stephensen and Rowatt, 1947; Goldstein and Goldstein, 1953). Animals use it for transmission of neural signals in brain, control of cell proliferation, growth and morphogenesis. Microorganisms use it for management of motility (Roshchina, 2010).

The synthesis of ACh is performed by an enzyme called choline acetyltransferase (ChAT). The discovery of ChAT comes much later than the discovery of ACh. The enzyme was first characterized by Nachmansohn and Machado in 1943. ChAT catalyzes the transfer of an acetyl group from the acetyl-CoA to choline, and produce ACh as a result. The enzyme is produced in the soma, and then transported to the nerve terminal. Therefore, ChAT is extensively used as a target gene for ISH experiments to localize cholinergic neurons. In this thesis research, the spatial distribution of cholinergic neurons were discovered through ChAT gene probes in ISH experiments.

2.1.2 Acetylcholine in the central nervous system of gastropod molluscs

ACh was extensively studied in the identified neurons of *Aplysia* because the giant neurons of *Aplysia*, similar to the neurons of Nudipleura, provides a useful platform for recording the electrical activity from single neurons. Giller and Schwartz (1968) investigated the regional

distribution of ChAT in the abdominal ganglion of *Aplysia* (Figure 12). Using ^{14}C-acetyl coenzyme A, ACh was synthesized and labeled; then the formation of the labeled ACh was readily detected. High rates of ACh synthesis was detected in different brain regions such as neuropil, pigmented cells, and bag cells, as well as in individual cells such as R14, L10, and R2.

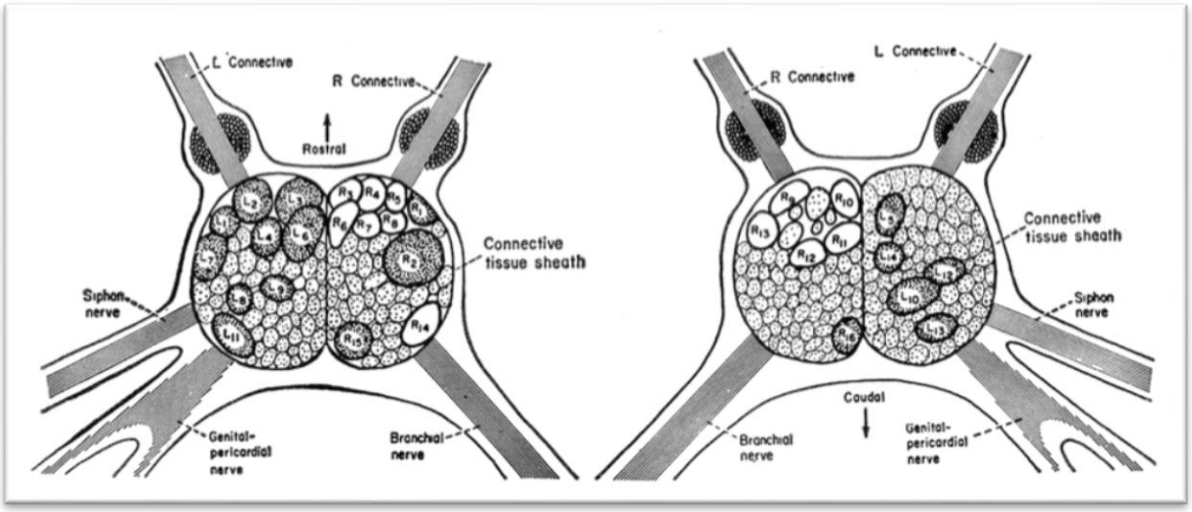

Figure 12 Cholinergic neurons in the abdominal ganglion of *Aplysia* (Giller and Schwartz, 1968)

Gardner and Kandel (1977) looked into the physiological and kinetic properties of cholinergic receptors in the identified interneurons of *Aplysia* buccal ganglia. They indicated the positions of the identified cholinergic neurons in a schematic drawing (Figure 13). The coloring of cells were determined according to the receptor types that they possess (Figure 2), where cells with slowly decrementing hyperpolarizing receptors are shown shaded in black; cells with depolarizing receptors are shown dotted, and cells that possess both depolarizing and rapidly decrementing hyperpolarizing receptors are shown half dotted and half striped. (Figure 13).

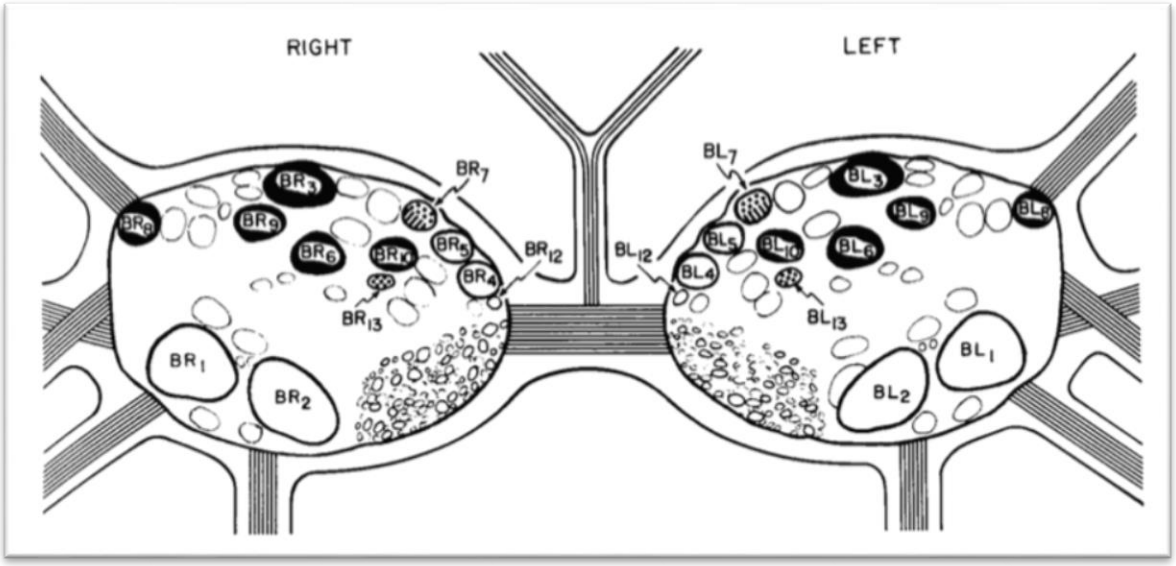

Figure 13 Cholinergic neurons in the buccal ganglion of *Aplysia* (Gardner and Kandel, 1977)

2.1.3 Si3 as a predicted cholinergic neuron in Dendronotus and Melibe

Cholinergic neurons have not been identified in any of the six nudipleuran species previously. However, a recent study that compare two nudibranch molluscs, *Dendronotus* and *Melibe*, found a neuron that is hypothesized to be cholinergic. The neuron was found to be a part of swim central pattern generator (CPG) network because its stimulation changed the activity of two homologous CPG neurons, swim interneuron 1 (Si1) and Si2 (Sakurai et al., 2011). Therefore, the neuron is named as Si3 (Sakurai, unpublished data). In *Dendronotus*, Si3 makes excitatory connection to Si2, whereas Si1 is inhibited by Si3 in *Melibe*. Moreover, these synapses are blocked by the nicotinic antagonist curare (Sakurai et al., unpublished data) (Figure 14), which implies that thepresynaptic neurons, Si3s, are cholinergic in both species. This hypothesis was tested in this study, by coupling ISH for ChAT gene with intracellular injection of a florescent label in Si3.

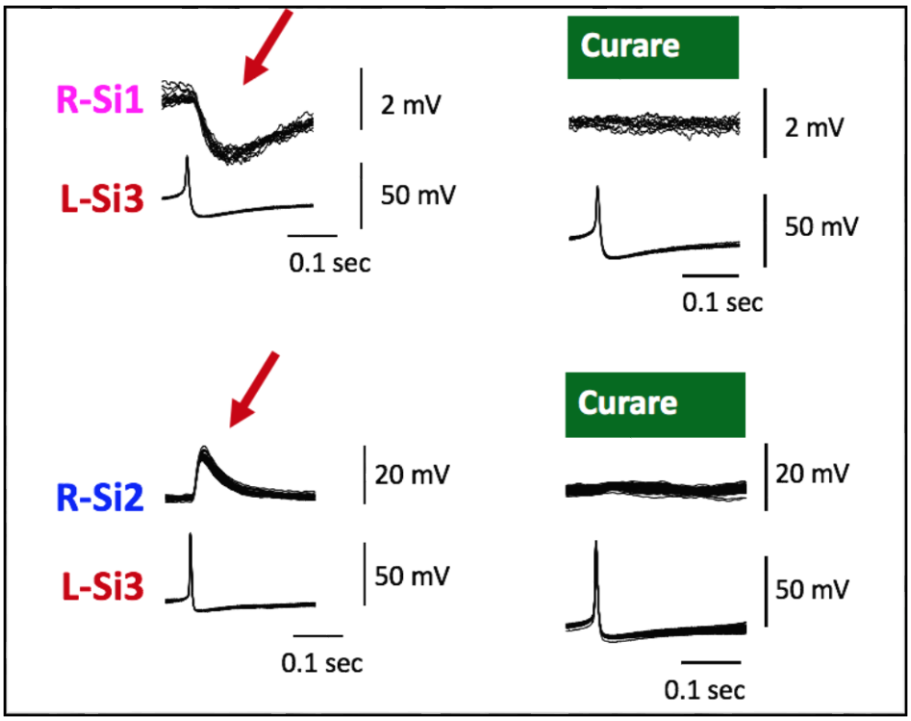

Figure 14 Simultaneous recordings from CPG neurons in *Melibe* and *Dendronotus* (Sakurai and Katz, unpublished results)

2.2 METHODS

2.2.1 BLAST searches

To find the sequence of ChAT gene in *Dendronotus* and *Melibe* species, the protein sequence of ChAT gene for *Aplysia* was extracted from the Uniprot protein sequence database (www.uniprot.org). Using this query sequence, BLAST searches were performed against *Dendronotus* and *Melibe* BLAST databases. The significant E values in the results indicated the ChAT genes in *Melibe* and *Dendronotus*. The fasta file was extracted from the database through blastdbcmd command.

2.2.2 Primer design for ChAT gene

Primers were designed using NCBI Primer Design tool (http://www.ncbi.nlm.nih.gov/tools/primer-blast), where optimum length of melting temperature was set to 62,5º C and optimum length of the primers was set to 26 bp. Primers were analyzed using the IDT Oligoanalyzer software (http://www.idtdna.com/analyzer/Applications/OligoAnalyzer) to determine the self-dimerization, hetero-dimerization, and hairpin formation characteristics.

DeChAT(537) F: CAACAGTGCTATTCTCTCGGACATTG

DeChAT(537) R: GTTAGCCCGTGGTGAATTTTGAAGTA

2.2.3 Animal dissection and brain removal

To anesthetize *Tritonia diomedea*, 1-Phenoxy-2-propanol (PP) is used. Animals were incubated in 12 mM PP (Wyetha, 2009) in artificial sea water (ASW) for 60-90 minutes depending on body size. *Dendronotus* and *Melibe* were anesthetized by injecting 0.33 M MgCl2 into the body cavity. The animal was positioned on the dissection tray with its dorsal surface of the body up. A cut was made near the buccal mass. All nerve roots around the brain were cut with fine scissors. Then the brain was removed and then transferred to a Sylgard lined dish that is filled with ASW Connective tissue surrounding the brain was removed under dissection microscope using forceps and fine scissors. Then the sheet surrounding the brain is removed carefully. The temperature was maintained at 4 °C during the process.

2.2.4 PCR

Polymerase chain reaction (PCR) was performed to amplify genes from complementary DNA (cDNA) or plasmid DNA using Taq DNA polymerase. The reactions were carried out with total volumes of 40 µL that includes: 4 µL of 10x Taq buffer (with KCl; Fermentas), 3 µL of 25 mM MgCl2 (Fermentas), 3 µL of 10 mM dNTP mix (10 mM each of dATP, dGTP, dCTP, and dTTP;

Fermentas), 0.5 μL of forward primer (at 10 μM), 0.5 μL of reverse primer (at 10 μM), 1-3 μL of template DNA, 0.4 μL of Taq DNA polymerase, and purified H_2O to 40 μL. The cycle was preceded by an initial denaturation at 95˚C for 90 sec, followed by 33 repetitions of the following cycles: denaturation at 95˚C (40 sec), annealing at a primer-specific temperature (40 sec), and elongation at 72˚C (1 min/kb). The final elongation was at 72˚C for 8 min. PCR products were visualized with UV light after gel electrophoresis, and then purified using a gel extraction kit (Qiagen).

2.2.5 Labeling of Si3

The some of Si3 were filled with 2 - 4% Neurobiotin Tracer (Vector Laboratories, Inc., Burlingame, CA) dissolved in 0.75 M KCl (pH 7.4), using an electrode that connected to an Axoclamp 2B amplifier. After neurobiotin injection, the brains were fixed for 14-24 hours in 4% formaldehyde in normal (1x) phosphate buffered saline (PBS) (Corning Life Sciences). After that, brains were incubated first in PBS about 60 minutes and then in 4% Triton X-100 in PBS for 10 minutes. This was followed by antiserum diluent (ASD, 0.5% Triton X-100, 1% normal goat serum and 1% bovine serum albumen in PBS), for about an hour for each of both. Then, Streptavidin-Alexa Fluor 594 conjugate (1:50 - 1:200, Invitrogen) was applied for 2-3 days.

2.2.6 in situ hybridization

The brain was fixed in 4% formaldehyde in 1x PBS for 14-22 hours at 4 °C. Then fixative was washed away by applying 1x PBS three times, for 5-15 mins each time. Typical washing steps were performed in 2D rotator with 25 rpm. To remove peripheral proteins, the brain was washed in PTW (0.1% Tween 20 in 1x PBS) (Fisher) for 15 min. In some cases, the brain was dehydrated in methanol before ISH. For dehydrations, it was washed with serial dilutions of PTW:methanol mixtures; for 10 minutes for each of 3:1, 1:1, and 1:3 mixtures. The brain was

then stored in 100% methanol at -20 °C until it was aimed to be used, for weeks or months. After methanol storage, rehydration is performed through incubating the brain in serial dilutions for 10 minutes for each of 1:3, 1:1, and 3:1 of PTW:methanol mixtures. Then the brain was washed in PTW for 10 min. After that, 0.3% Triton X 100 (Fisher) was applied for 10 min, followed by a 5 min PTW wash. For some cases, TEA HCl and acetic anhydride was applied to make the membrane more permeable. For this step, the brain was washed twice quickly in TEA HCl (pH: 8.0) (Sigma) and then in 1 ml of TEA HCl with 2.5 µl of acetic anhydride (Sigma) two times for 5 min each. Then, the brain was washed with PTW four times. Since the brain was already desheated, no protease was applied.

After these membrane treatments, hybridization step was started. Typically, 0.4 mL hybridization buffers were prepared for each brain, including 50% formamide (Sigma), 5 mM EDTA (Invitrogen), 5x SSC (Roche), 1x Denhardt's solution (USB), 0.1% Tween 20, and 2 mg/ml yeast tRNA (Invitrogen). 50-100 ul DNA probes with 20-40 mg/ul concentrations were added to 0.4 mL hybridization buffer. The hybridization was performed at 52˚C for 14 –18 hours on a 3D shaker with 12 rpm. Post-hybridization washes were performed with a solution containing 50% formamide, 5x SSC, and 1% SDS at 50˚C for 1 hour, and then with 0.2x SSC for another hour. After several quick washes with PBT, the brain was incubated in 10% normal goat serum (Sigma) in PBT for 60 minutes at 4oC on a 3D rotator. Antibody labeling was performed in 1:1000 alkaline phosphatase-conjugated DIG antibodies (Roche) in 1% goat serum in PBT on a shaker at 4˚C for 16-18 hours. Then the brain was washed in PBT four times at room temperature, for 2-3 hours in total. The brain was then washed in detection buffer (100 mM NaCl, 50 mM MgCl2, 0.1% Tween 20, 1 mM Tetramisol HCl (Sigma), and 100 mM Tris HCl at a pH of 9.5) three times for one hour. At the final step, labeling was detected using 40 µl of

NBT/BICP solution (Roche) to 1.5 ml of detection buffer in the dark. Typical waiting times for color development was 6-15 minutes. The reaction was stopped with PBS and images of the brain were taken.

2.3 RESULTS

In situ hybridization (ISH) experiments were performed on whole mount brains of *Melibe* and *Dendronotus*. The cholinergic neurons were visualized in purple color through alkaline phosphatase color reaction, where the intensity of the color in a labeled cell is expected to correlate with the quantity of the labeled gene in the cell. ChAT gene probes labeled three cells in each pleural ganglion of *Dendronotus*, and up to two cells in each cerebral ganglion. *Melibe* also had 3 cells in each pedal ganglion and 7-8 cells in each pleural ganglion (Figure 15).

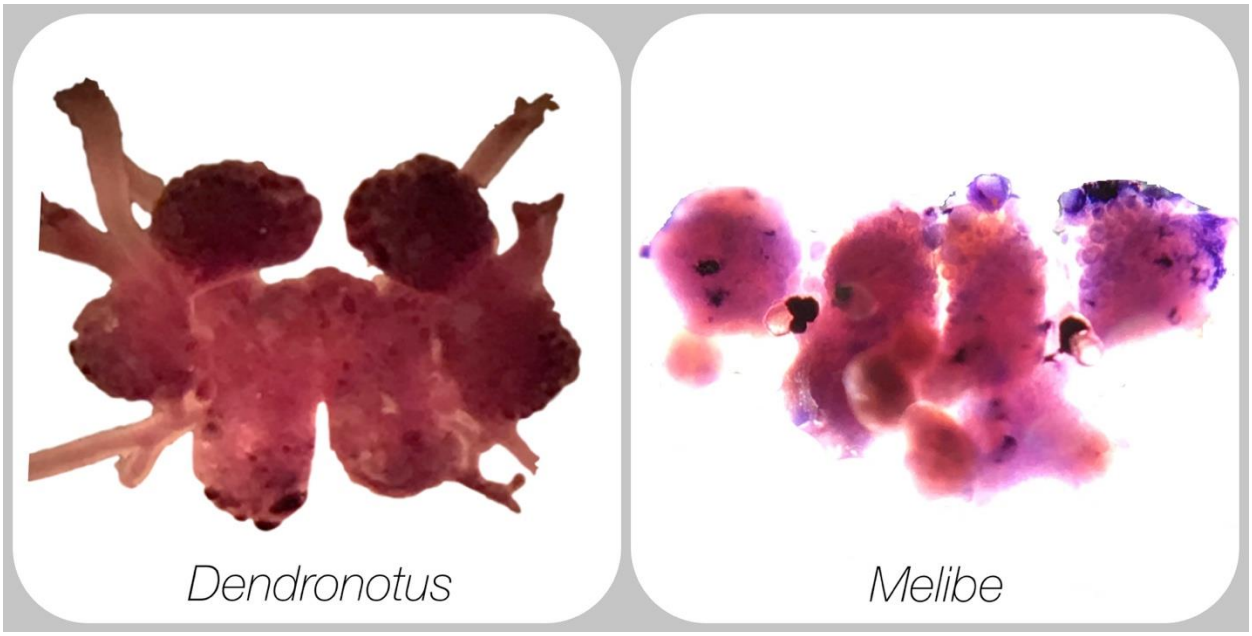

Figure 15 Whole mount DIG-ISH on *Dendronotus* and *Melibe* CNS

In the second round of experiments, it was aimed to determine if any of these labeled cells is Si3. To achieve this goal, Si3s were filled with biotin through glass electrodes, and fluorescently labeled with streptavidin. After that, whole mount ISH experiments were performed on the same brain and then overlap of the two labels was analyzed. Figure 16 shows the whole mount *Dendronotus* brain before and after ChAT labeling. The dark points indicates the soma of the cells that are laveled with ChAT, and the two bright dots in both images shows left and right Si3. In Figure 17, the area around left and right Si3 on the same brain is shown in a close-up image. The same section of the brain was pictured under light microscopy and fluorescent microscopy, as shown in the left and right sides of Figure 17 respectively. As the red arrows points out in the figure, Si3s were only slightly labeled with DIG probes because intensity of dark color on both Si3s was very low.

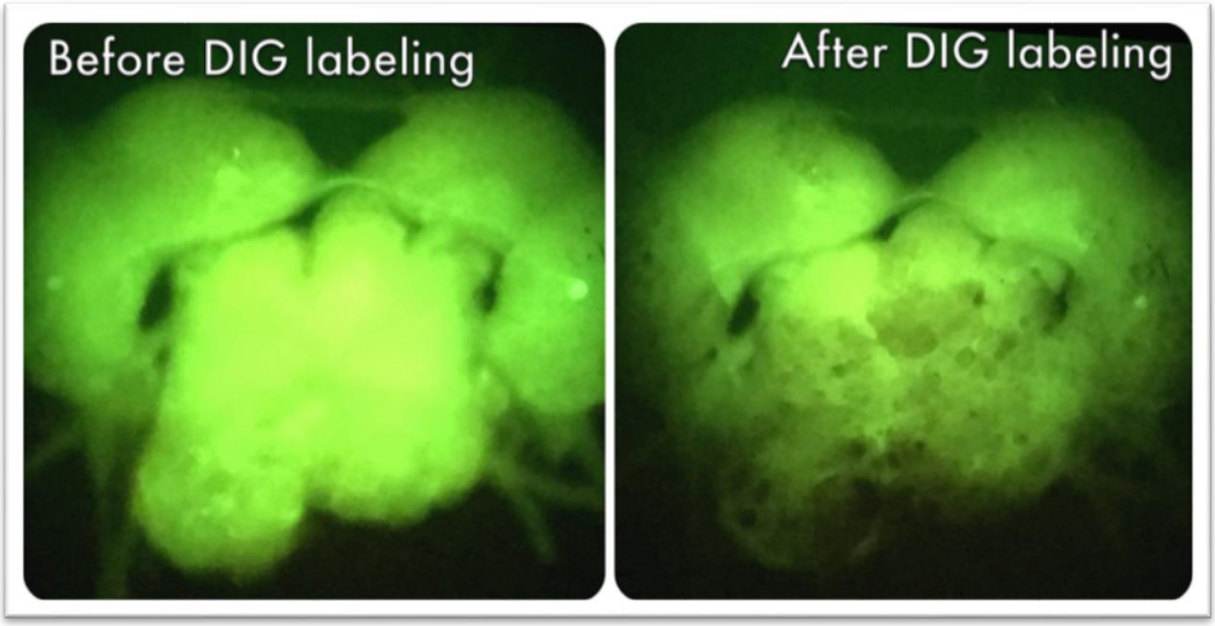

Figure 16 ChAT DIG ISH on whole-mount *Dendronotus* brain where Si3s were fluorescently labeled

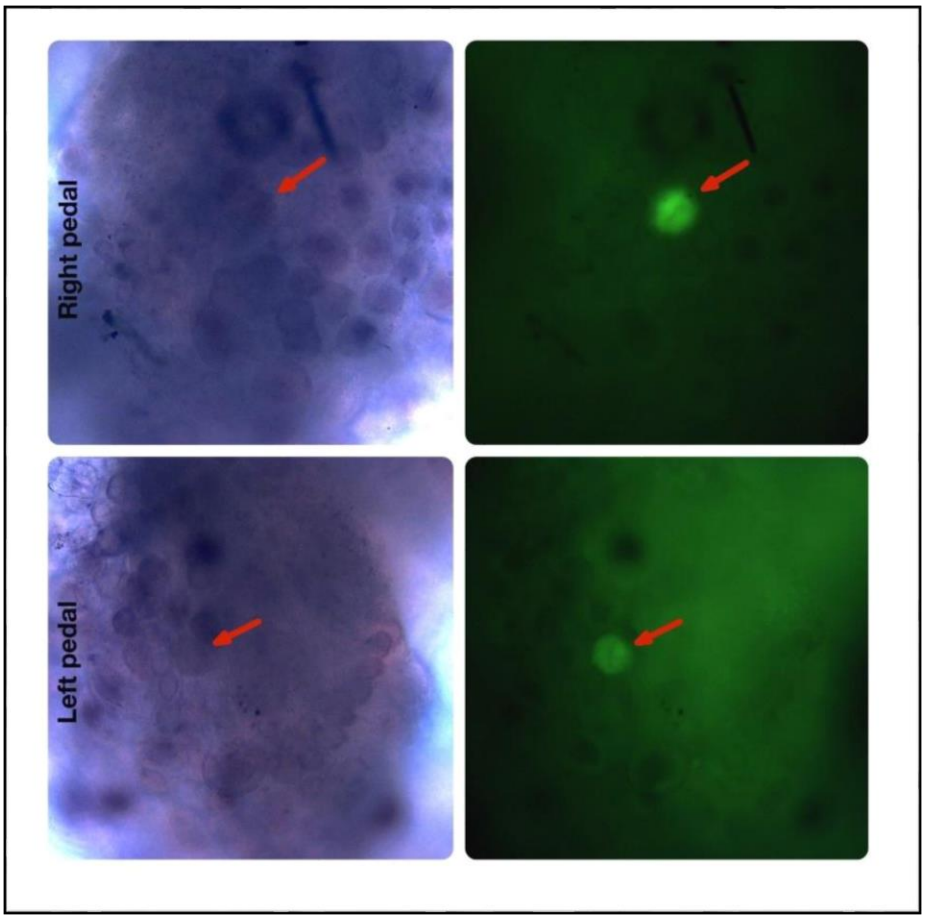

Figure 17 ChAT DIG ISH on whole-mount *Dendronotus* brain where Si3s were fluorescently labeled.

The same brain section was pictured under light microscopy (left) and fluorescent microscopy (right). The red arrows point out Si3s.

2.4 DISCUSSION

Previous studies showed that there are a large number of cholinergic neurons in *Aplysia* CNS. Therefore, it was hypothesized that gastropod molluscs, including the six nudipleurans studied in this thesis, have many cholinergic neurons in their CNSs. As expected, whole mount ISH

experiments labeled many cells in the whole mount brains of *Dendronotus* and *Melibe* (Figure 15).

In the double labeling experiment, the Si3s were successfully labeled fluorescently. The DIG whole mount experiments were also successfully conducted. However, Si3s were only slightly labeled and it was not clear whether this is a background labeling or a real labeling. In the colorimetric labeling reactions, such as DIG & alkaline phosphatase labeling that is utilized here, the color intensity of labeling is affected by time duration of visualization. In the ISH experiments that were performed in this study, the color development was stopped after 8-10 min by removal of alkaline phosphatase buffer. If more time was provided for color development, the Si3 might possibly be labeled darker.

The goal of determining whether Si3 is cholinergic in *Melibe* and *Dendronotus* could also be achieved in alternative ways, other than ISH. For example, after isolating Si3 from brain using fine forceps and scissors, quantitative PCR (qPCR) experiment could be performed for ChAT gene to determine the quantity of ChAT in the cell. Alternatively, the presence of ChAT enzyme could be checked through injecting labeled acetyl CoA into Si3 and examining the release of newly formed labeled ACh in synaptic cleft.

On the other hand, it might be the case that the post-synaptic neurons at the two identified synapses of *Melibe* and *Dendronotus* are gated by nicotine but not ACh, as White et al. (2014) suggested. In this case, the blockage of the synapses by curare, a nicotinic inhibitor, does not make the pre-synaptic neurons, Si3s, cholinergic. Therefore, pursuing additional molecular experiments that target ChAT would not be worthy after getting negative implications for the presence of ChAT in Si3. Additional gene markers can be inspected to find out whether Si3 in *Dendronotus* is homologous to Si3 in *Melibe*.

3 CONCLUSION AND FUTURE PERSPECTIVES

In this thesis, an extensive analysis of molluscan nAChR subunits has been performed. In total, 123 subunit sequences, including 24 nAChR subunit classes in six nudipleuran species, have been identified and annotated. An inventive methodology was used for identifying orphan genes and de-orphanizing them. The major evolutionary relationships between subunits were clarified. The relative mRNA expression levels of each subunit showed surprising differences. Cholinergic neurons are localized in the CNS of two nudipleurans. A particular cell in *Dendronotus* was further analyzed to assess the presence of ChAT.

In the future, single cell RNA-Seq experiments could be performed to investigate the expression of AChR subunits and ChAT in identified single neurons in CPG neural networks of nudipleurans. Through this way, the potency of receptor subunit composition on the electrical activity of neural networks could be investigated. In general, such studies can provide a better comprehension of how neurochemistry influence nervous system function.

REFERENCES

Boorman JPB, Groot-Kormelink PJ, Sivilotti LG. 2000. Stoichiometry of human recombinant neuronal nicotinic receptors containing the b3 subunit expressed in *Xenopus oocytes*. J Physiol 529(Pt 3), 565– 577.

Boulter J, Connolly J, Deneris EDG, Heinemann S. 1987. Functional expression of two neuronal nicotinic acetylcholine receptors from cDNA clones identifies a gene family. Proc Natl Acad Sci USA 84, 7763–7777.

Changeux J, Edelstein SJ. 2001. Allosteric mechanisms in normal and pathological nicotinic acetylcholine receptors. Curr Opin Neurobiol 11, 369 –377.

Charif D, Lobry JR. 2007. SeqinR 1.0-2: a contributed package to the R project for statistical computing devoted to biological sequences retrieval and analysis. In Structural approaches to sequence evolution (pp. 207-232). Springer Berlin Heidelberg.

Chemeris NK, Kazachenko VN, Kislov AN, Kurchikov AL. 1982. Inhibition of acetylcholine responses by intracellular calcium in *Lymnaea stagnalis* neurones. J Physiol 323, 1–19.

Chiarandini DJ, Gerschenfeld HM. 1967. Ionic mechanism of cholinergic inhibition in molluscan neurons. Science 156, 1595–1596.

Chiarandini DJ, Stefani E, Gerschenfeld HM. 1967. Ionic mechanism of cholinergic excitation in molluscan neurons. Science 156, 1597–1599.

Dale HH. 1914. The action of certain esters and ethers of choline, and their relation to muscarine. J Pharmacol 6, 147-190.

Deneris ES, Connolly J, Boulter J, Wada E, Wada K, Swanson LW, Patrick J, Heinemann S. 1988. Primary structure and expression of β2: a novel subunit of neuronal nicotinic acetylcholine receptors. Neuron 1, 45–54.

Duguid JR, Raftery MA. 1973. Fractionation and partial characterization of membrane particles from *Torpedo californica* electroplax. Biochemistry 12, 3593-3597.

Elgoyhen AB, Vetter DE, Katz E, Rothlin CV, Heinemann SF, Boulter J. 2001. α10: a determinant of nicotinic cholinergic receptor function in mammalian vestibular and cochlear mechanosensory hair cells. Proc Natl Acad Sci USA 98, 3501–3506.

Fertuck HC, Salpeter MM. 1974. Localization of acetylcholine receptor by ^{125}I-labeled α-bungarotoxin binding at mouse motor endplates. Proc Natl Acad Sci 71, 1376-1378.

Gardner D, Kandel E. 1977. Physiological and kinetic properties of cholinergic receptors activated by multiaction interneurons in buccal ganglia of *Aplysia*. J Neurophysiol 40, 333-348.

Giller E, Schwartz JH. 1968. Choline acetyltransferase: regional distribution in the abdominal ganglion of *Aplysia*. Science 161, 908-911.

Goodheart JA, Bazinet AL, Collins AG, Cummings MP. 2015. Relationships within Cladobranchia (Gastropoda: Nudibranchia) based on RNA-Seq data: an initial investigation. R Soc Open Sci 2, 150196.

Gotti C, Clementi F. 2004. Neuronal nicotinic receptors: from structure to pathology. Prog Neurobiol 74, 363–396.

Hille B. 2001. Ionic channels of excitable membranes. Sinauer, Sunderland, MA, 3rd Ed, p 814.

Hogg RC, Raggenbass M, Bertrand D. 2003. Nicotinic acetylcholine receptors: from structure to brain function. Rev Physiol Biochem Pharmacol 147, 1–46.

Karlin A. 2002. Emerging structure of the nicotinic acetylcholine receptors. Nature Reviews Neurosci 3, 102-114.

Kawashima K, Misawa H, Moriwaki Y, Fujii YX, Fujii T, Horiuchi Y, Yamada T, Imanaka T, Kamekura M. 2007. Ubiquitous expression of acetylcholine and its biological functions in life forms without nervous systems. Life Sci 80, 2206–2209.

Kumar S, Stecher G, Tamura K. 2016. MEGA7: Molecular Evolutionary Genetics Analysis version 7.0 for bigger datasets. Mol Biol Evol, msw054.

Li B, Dewey CN. 2011. RSEM: accurate transcript quantification from RNA-Seq data with or without a reference genome. BMC bioinfo 4, 12:1.

Lillvis JL, Gunaratne CA, Katz PS 2012. Neurochemical and neuroanatomical identification of central pattern generator neuron homologues in Nudipleura molluscs. PLoS One 7, e31737.

Lindstrom J. 1997. Nicotinic acetylcholine receptors in health and disease. Mol Neurobiol 15, 193–222.

McGinnis S, Madden TL. 2004. BLAST: at the core of a powerful and diverse set of sequence analysis tools. Nucleic Acids Res 32, W20-25.

Nachmansohn D, Coates CW, Rothenberg MA. 1946. Studies on cholinesterase II. Enzyme activity and voltage of the action potential in electric tissue. J Biol Chem 163, 39-48.

Newcomb JM, Sakurai A, Lillvis JL, Gunaratne CA, Katz PS. 2012. Homology and homoplasy of swimming behaviors and neural circuits in Nudipleura molluscs. Proc Natl Acad Sci USA 109, 10669-10676.

Paradis E, Claude J, Strimmer K. 2004. APE: analyses of phylogenetics and evolution in R language. Bioinformatics 20, 289-290.

Raftery MA, Hunkapiller MW, Strader CD, Hood LE. 1980. Acetylcholine receptor: complex of homologous subunits. Science 208, 1454-1456.

Reed JK, Raftery MA. 1976. Properties of the tetrodotoxin binding component in plasma membranes isolated from *Electrophorus electricus*. Biochem 15, 944-953.

Sadamoto H, Takahashi H, Okada T, Kenmoku H, Toyota M. 2012. *De novo* sequencing and transcriptome analysis of the central nervous system of mollusc *Lymnaea stagnalis* by deep RNA sequencing. PLoS One 7, e42546.

Sakurai A, Katz PS. 2013. Homologues of interneurons in two different species have distinct functions in the generation of similar rhythmic motor patterns. Soc Neurosci Abstr, San Diego 169.01.

Sakurai A, Gunaratne CA, Katz PS. 2014. Two interconnected kernels of reciprocally inhibitory interneurons underlie alternating left-right swim motor pattern generation in the mollusk *Melibe leonina.* J Neurophysiol 112, 1317-1328.

Sakurai A, Newcomb JM, Lillvis JL, Katz PS. 2011. Different roles for homologous interneurons in species exhibiting similar rhythmic behaviors. Curr Biol 21, 1036-1043.

Saitou N, Nei M. 1987. The neighbor-joining method: a new method for reconstructing phylogenetic trees. Molec Biol Evol 4, 406-425.

Schmidt J, Raftery MA. 1973. Purification of acetylcholine receptors from *Torpedo californica* electroplax by affinity chromatography. Biochem 12, 852-856.

Senatore A, Edirisinghe N, Katz PS. 2015. Deep mRNA sequencing of the *Tritonia diomedea* brain transcriptome provides access to gene homologues for neuronal excitability, synaptic transmission and peptidergic signaling. PLoS One 10, e0118321.

Stroud RM. 2008. Michael A. Raftery (1936–2007) - the first enzyme mechanism, sequential cooperativity, and the nicotinic acetylcholine receptor defined. Protein Sci 17, 1864-1866.

Team RC. 2013. R: A language and environment for statistical computing.

Tsunoyama K, Gojobori T. 1998. Evolution of nicotinic acetylcholine receptor subunits. Mol Biol Evol 15, 518– 527.

van Nierop P, Bertrand S, Munno DW, Gouwenberg Y, Van Minnen J, Spafford JD, Syed NI, Bertrand D, Smit AB. 2006. Identification and functional expression of a family of nicotinic acetylcholine receptor subunits in the central nervous system of the mollusc *Lymnaea stagnalis*. J Biol Chem 281, 1680-1691.

van Nierop P, Keramidas A, Bertrand S, van Minnen J, Gouwenberg Y, Bertrand D, Smit AB. 2005. Identification of molluscan nicotinic acetylcholine receptor (nAChR) subunits involved in formation of cation- and anion-selective nAChRs. J Neurosci 25, 10617–10626.

Venter JC, di Porzio U, Robinson DA, Shreeve SM, Lai J, Kerlavage AR, Fracek SP, Jr, Lentes KU, Fraser CM. 1988. Evolution of neurotransmitter receptor systems. Prog Neurobiol 30, 105–169.

Vulfius EA, Veprintzev BN, Zeimal EV, Michelson MJ. 1967. Arrangement of cholinreceptors on the neuronal membrane of two pulmonate gastropods. Nature 216, 400-401.

Vulfius CA, Tumina OB, Kasheverov IE, Utkin YN, Tsetlin VI. 2005. Diversity of nicotinic receptors mediating Cl- current in *Lymnaea* neurons distinguished with specific agonists and antagonist. Neurosci Lett 373, 232–236.

White SH, Carter CJ, Magoski NS. 2014. A potentially novel nicotinic receptor in *Aplysia* neuroendocrine cells. J Neurophysiol 112, 446–462.

Zuckerkandl E, Pauling L. 1965. Evolutionary divergence and convergence in proteins. Evol Genes Proteins 97, 97-166.

APPENDICES

Appendix A. R CODES

Appendix A.1 Bootstrap analysis in R

```
install.packages("phangorn")
install.packages("ape")
library(ape)
library(phangorn)
setwd("~/Desktop/MEGA")
phyd = read.phyDat("Melibe22sub.fas", type= "AA", format = "fasta")
dm <- dist.logDet(phyd)
tr <- NJ(dm)
fit <- pml(tr, phyd)
treeMP <- pratchet(phyd)
treeMP <- acctran(treeMP, phyd)
set.seed(123)
BStrees <- bootstrap.phyDat(phyd, pratchet, bs = 1000)
treeMP <- plotBS(treeMP, BStrees, "unrooted",p=0)
```

Appendix A.2 Plot of hierarchical clustering in R

```
install.packages("seqinr")
install.packages("ape")
install.packages("RColorBrewer")
library(seqinr)
library(ape)
library(RColorBrewer)
SAln = read.alignment(‘‘My_Aln.fasta", format = "fasta")
SDist = dist.alignment(SAln, matrix = "identity")
hc <- hclust(SDist, method="ward.D2")
phy = as.phylo(hc)
```

```
add.scale.bar(length = 0.1)
clus19 = cutree(hc, 19);
mypal =
c(brewer.pal(8,"Dark2"),"#1f78b4","#6a3d9a","#33a02c","#a50026","#000000",
"#ff0074", "#6ab7fd", "#fa9fb5", "#636363", "#33577c", "#f03b20",
"#bd6969", "#1a2865", "#c51b8a")

plot(phy, type = "fan", tip.color = mypal[clus4],cex=0.5)
```

Appendix A.3 Plot of RSEM Tree

```
myData = read.csv("~/Desktop/myData.csv", row.names=1)
hc = hclust(dist(myData, method="euclidean"),method="mcquitty")
plot(as.phylo(hc),cex=1)
```

Appendix B BLAST Command Line Scripts

Appendix B.1 BLAST Analyses

```
module load BioInformatics/ncbi-blast-2.2.31+

makeblastdb -in ~/SP00011553/Vela_Backup/Transcriptomes/MeliTSAFLT.fasta -
dbtype nucl -out MelDB -parse_seqids

tblastn -db ~/SP00011553/seyda/blastDB/PleDB -query
Aplysia20subunits.fasta -outfmt 7 -evalue 1e-80

blastdbcmd -db
~/SP00011553/Vela_Shared_pkatz/BlastDBs/Molluscs/MelibeTSAFLT/MeliTSAT -
entry comp63127
```

Appendix B.2 EMBOSS Translation

```
module load BioInformatics/Emboss6.3.1
transeq nucleotides.txt translations.pep -frame=6
```

Appendix C LINUX SCRIPTS

```
for files in *.txt; do sed 's/_seq[1-9]//' $files>new; mv new $files; done
```

Appendix D. SCP Expression

When setting up a protocol for ISH experiments, a gene that is known to be abundantly expressed was aimed to be targeted. SCP, as being the second most abundant secreted peptide in the nudipleuran CNS (Senatore et al., unpublished data), was found appropriate for initial ISH experiments. ISH experiment was performed on *Tritonia* brain with SCP gene probes. A cluster of linearly aligned cells was found in the dorsal cerebral ganglia of *Tritonia* (Figure 18A). Cerebral ganglia showed the highest degree of SCP expression. The SCP-positive cells in the pleural ganglion was scattered. In the ventral side (Figure 18B), a cluster of cells near the connection between right pedal and right cerebral were labeled with SCP probe. Additional cells in pleural and cerebral ganglia were found to express SCP. The primer sequences that were used in the experiments are provided below.

SCP(343)F: CTGTCTCTCTGACGCTTCTCTTTGTC

SCP((343)R: TAAGAGCTTGGGTACATTTTCGAGACG

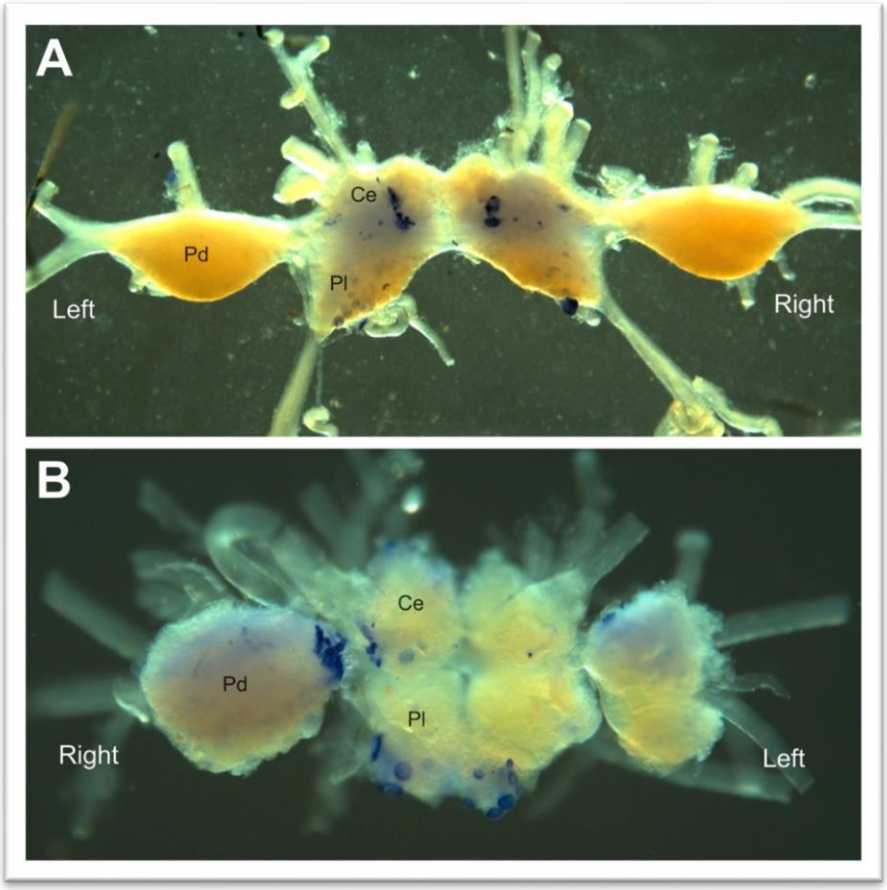

Figure 18 SCP ISH on *Tritonia*

(A) SCP ISH results on dorsal side of a Tritonia brain. (B) SCP ISH results on ventral side of another Tritonia brain. Pedal, cerebral and pleural ganglia are labeled as Pd, Ce, and Pl on the image.